

A spatially constrained QCD colour reconnection in pp, pA, and AA collisions in the PYTHIA8/Angantyr model

Leif Lönnblad and Harsh Shah

Dept. of Physics, Lund University, Sölvegatan 14A, Lund, SE-223 62, Sweden.

Contributing authors: leif.lonnblad@hep.lu.se; harsh.shah@hep.lu.se;

Abstract

We present an updated version of the QCD-based colour reconnection model in PYTHIA8, where we constrain the range in impact parameter for which reconnections are allowed. In this way, we can introduce more realistic colour reconnections in the Angantyr model for heavy ion collisions, where previously only reconnections within separate nucleon sub-collisions have been allowed. We investigate how the new impact parameter constraint influences final states in **pp** collisions, and retune parameters of the multi-parton interaction parameters in PYTHIA to compensate so that minimum bias data are reproduced. We also study multiplicity distributions in **pA** collisions and find that, in order to counteract the loss in multiplicity due to the introduction of global colour reconnections, we need to modify some parameters in the Angantyr model while keeping the parameters tuned to **pp** fixed. With Angantyr we can then extrapolate to **AA** collisions without further parameter tuning and retaining a reasonable description of the basic multiplicity distributions.

Keywords: Colour reconnection, PYTHIA8/Angantyr, Heavy-ion collision

1 Introduction

The field of heavy-ion (HI) collisions is widely studied under assumption of the creation of a thermalised medium of strongly coupled partons; the Quark-Gluon-Plasma (QGP). Observables showing, *e.g.*, *strangeness enhancement*, long range *collectivity*, *quarkonia suppression*, and *jet quenching* in HI collisions are conventionally assumed to reflect the formation of such a QGP [1]. Two of these observables, namely *strangeness enhancement* [2], and long range *collectivity* [3], are, however, observed also in pp collisions, where the QGP formation is conventionally not assumed to be present. This has cast doubts on our understanding of pp collisions as well as on our understanding of these observables in HI collisions.

PYTHIA [4, 5] is a well known and widely used event generator for small collision systems such as e^+e^- and pp. In [6] we developed the Angantyr model to allow the use of PYTHIA's excellent description of pp collisions also for HI, by introducing a sophisticated stacking of multiple pp-like collisions to build up complete HI collision events. In this way, we have constructed a test bench for developing models for collective effects that can explain the behaviour of the above-mentioned observables without introducing a QGP.

Angantyr uses an advanced Glauber model [7, 8], where the Good-Walker picture [9] of diffraction provides a description of fluctuations (often referred to as Glauber-Gribov colour fluctuations) that influences both the number of nucleon-nucleon (NN) sub-collisions and the type of each individual sub-collision in a heavy-ion

event. Each of these sub-collisions is then simulated using the standard PYTHIA minimum-bias machinery, producing non-diffractive, elastic, single and double diffractive sub-events according to the type determined in the Glauber simulation. The resulting sub-events are then simply stacked together into a full HI event.

In Angantyr there is a special treatment of situations where one nucleon collides non-diffractively with several others. In this situation only one such sub-collision is considered *primary* and is modelled by a full non-diffractive event in PYTHIA. The other, *secondary*, pp collisions are treated as diffractive excitations of the additional nucleon and modelled in PYTHIA using the standard Pomeron-based single diffractive model. In such a secondary non-diffractive (SND) sub-collision there is a special treatment of the Pomeron parton densities, to better mimic the particle production of a non-diffractive pp event in the direction of the excited nucleon.

The Angantyr model contains a number of new parameters, however most of these are tuned using pp observables, except the ones controlling the SND sub-events, which are tuned to pA observables. It is an important feature of the Angantyr model that there is then no further parameters to tune when generating AA collision events. The Angantyr model is nevertheless able to reproduce general features such as multiplicity distributions in different centrality bins for, *e.g.*, PbPb and XeXe collisions at the LHC.

Currently, although the sub-events are generated on parton-level and stacked together to be hadronized together using PYTHIA string fragmentation, the colour dipoles that build up the string from different sub-collisions do not interact with each other in the Angantyr model. Therefore in the Angantyr all sub-collisions hadronize separately in HI events. Figure 1 outlines the general scheme of the existing HI events simulation in the left part under PYTHIA8/Angantyr (Default). This is, of course, a simplification and we don't believe that there is no cross-talk at all between the sub-events.

This work is aimed to further develop the Angantyr model to have interactions among partons produced in different sub-collisions in HI events. Recently two models based on *string interaction* have been investigated by the Lund group.

One is the shoving model [10, 11], where the overlapping fields of nearby strings give a repulsive force that gives rise to an azimuthal flow. The other is the rope hadronization model [12, 13] where the increased tension in overlapping strings gives rise to strangeness enhancement. In addition there is now a model for hadron rescattering in PYTHIA8 [14, 15], that also works for HI collisions.

Here we will instead focus on how the strings are formed from the coloured partons produced in the scattering and after initial- and final-state parton showers. This is typically done using the $N_c \rightarrow \infty$ limit where any coloured parton is uniquely coupled to an anti-coloured one in a *dipole*. Gluons carry both colour and anti-colour, so we will get a set of dipoles connected together with gluons that form strings.

PYTHIA treats multi-parton interactions (MPIs) [16] as independent partonic interactions, where the initial- and final-state parton showers are also independent vacuum radiations. Before the produced strings are allowed to hadronize, however, it was early on clear that the strings in these different parton interactions needed to undergo a *colour reconnection* (CR) procedure in order to describe pp data.

Colour reconnections is the only step in PYTHIA where the produced partons from different sub-scatterings interact with each other before hadronization. In that spirit, we will here look at the effects of allowing CR to work also on partons from different NN sub-collisions in HI collisions as illustrated on the right side of Figure 1 under PYTHIA8/Angantyr (new).

In this work we use the QCD-CR model [17], which is different from the MPI-based CR model [16], which is the default CR model in PYTHIA8. We give a short overview of the two CR models in section 2. We introduce a new parameter to determine the allowed spatial transverse separation between colour dipoles to be colour reconnected. This new parameter plays a key role in enabling CR among partons from different sub-collisions. We describe its importance and expected effects on the event final states in more detail in section 2.1.

The rest of this paper is organised as follows. In section 3 we discuss the re-tuning of selected parameters needed for the reproduction of pp collision data to remain intact when we introduce the transverse separation cut. There we also describe

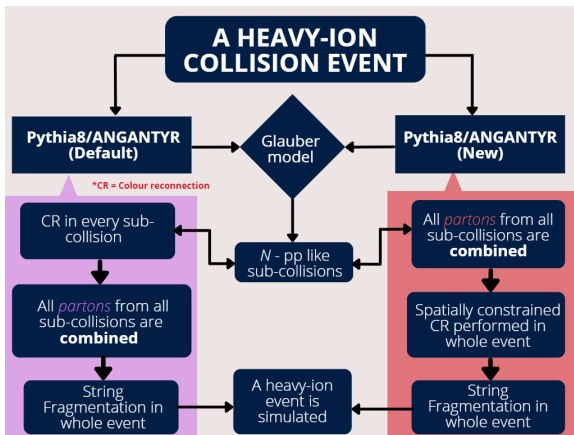


Fig. 1: Comparison of the new implementation against the default structure of the event simulation in the Angantyr model. So far we were treating a heavy-ion collision event as a sophisticated superposition of multiple pp like collisions stacked together at the parton level after the colour reconnection. In this work, we are treating a heavy-ion event as one event as early as possible, which is from the colour reconnection state onward.

the subsequent re-tuning of SND parameters to reproduce multiplicity distributions in pPb data. We also introduce some modifications to the fragmentation of so-called junction strings in PYTHIA8 (explained in more detail in appendix A), which were necessary to allow QCD-CR in HI collisions. In section 4 we present some outcomes of the new model in pp, pA, and AA, before we present our conclusions in section 5 together with an outlook.

2 The Colour Reconnection

In hadronic collisions there are coloured particles in both the initial and final state, and it is reasonable to assume that there will be multiple parton scattering in a single collision. Assuming that all scatterings are completely independent of each other, and also contribute equally to the momentum distribution and multiplicity of final state hadrons, one would expect that the multiplicity would grow with the number of scatterings, while observables such as the average transverse momentum, $\langle p_{\perp} \rangle$, would be almost constant.

The fact that already the ISR [18] and UA1 [19] experiments found that $\langle p_{\perp} \rangle$ actually

increases with the number of charged particles, N_{ch} , tells us that this picture of MPIs is too naive, and indicates some sort of collective behaviour in the hadronization stage, that correlates partons from different scatterings. In particular it would indicate that additional scatterings would contribute to the average transverse momentum but not so much to the multiplicity.

In the original MPI model [16] this was handled with a colour rearrangement. A single partonic scattering would produce colour connections between scattered partons and the hadron remnants, resulting in long strings that produce many (soft) hadrons. A secondary scattering would naively do the same, but the rearrangement allows the secondary scattered partons to instead be connected to the previous scatterings. This reduces the number of additional soft hadrons produced in additional scatterings. The scatterings will, however, still contribute to the average transverse momentum, giving a rise in $\langle p_{\perp} \rangle$ with multiplicity.

Later the effects of colour rearrangements were also studied in particle event generators in a series of papers [20–24] to investigate possible CR in e^+e^- annihilation at LEP. One of the problems was understanding the uncertainty in the W mass as measured in $e^+e^- \rightarrow W^+W^- \rightarrow q_1\bar{q}_1'q_2\bar{q}_2'$ events. The naive expectation is here that the $q\bar{q}$ from each W -decay are colour connected separately. However, it is possible to have an alternative configuration where quarks and anti-quarks originating from different W bosons are colour connected as the final colour configuration. The difference in colour connections will influence the jet shapes, and hence also the experimentally reconstructed W masses. The probability for such a rearrangement of the colour configuration is given by $1/N_c^2 = 1/9$. It is referred as *colour reconnection* in the event generators. Today, in event generators such as PYTHIA, CR is a generic name given to algorithms which decide a colour configuration to be used to colour connect the partons. The probability for CR in lepton collisions is further reduced by the limited space-time overlap between the produced parton systems from the W bosons decays in the case of the above example, as described in [21].

Due to the non-perturbative nature and limited understanding of the colour configuration at the parton level, there is some liberty in developing CR models. The common approach in all of

them is minimizing the rapidity span of the produced hadrons from the strings. For more details, we refer to [16, 17] and references therein.

The possibility of a CR model based on $SU(3)$ colour algebra with a finite number of colours was first proposed in [20] for the W pair production and their purely hadronic decays in e^+e^- collisions. The QCD-CR model [17] is an extension of the default CR in PYTHIA introducing $SU(3)$ colour algebra in pp collisions. In addition to the standard reconnection of colour lines (sometimes referred to as a *swing*, see Figure 2a), this model also includes the possibility for *junction* formation, where three string pieces are connected to a single point. Junctions can be formed by two dipoles reconnecting into a junction–anti-junction pair connected by a new colour line as in Figure 2b, or by three dipoles reconnecting to separate junction–anti-junction systems as in Figure 2c. As the junctions carry baryon number, the QCD-CR model introduces a new baryon production mechanism, in addition to the normal formation of baryons in the string fragmentation through diquark production.

Before we discuss junctions and other possibilities for colour reconnection under QCD-CR, let us see what makes it beyond the leading colour (LC). Referring to the arguments in [17], consider a scenario when two gluons are extracted from a proton, here QCD gives several possibilities for the colour multiplets formed by these two gluons. Each of the gluons can have 8 possible colours, and from the colour algebra, these two gluons are in one of the colour multiplets,

$$8 \otimes 8 = 27 \oplus 10 \oplus \bar{10} \oplus 8 \oplus 8 \oplus 1.$$

The 27 (or a "viginti-septet") represents LC, where the two gluons extend four independent strings from the proton. For random gluon colours, this has the probability

$$P_{LC} = \frac{27}{64} \approx 0.4,$$

which is less than 50%. Hence it is evident that sub-leading colour topology has non-negligible effects. We note that the least probable colour configuration is 1 (singlet), where both gluons have exactly opposite colours, and it can occur with a probability of 1/64. Similarly, other possible cases

of two quarks, a quark and a gluon, or a quark and an anti-quark are shown in [17]. The conclusion is that sub-leading multiplets are ignored in a LC model, and for hadron collisions, sub-leading multiplets have a significant contribution. The colour algebra becomes more and more complex for cases where multiple partons are extracted from the beam particle.

The QCD-CR starts with LC ($N_c \rightarrow \infty$) connections after the parton showers and assigns $SU(3)$ weighted colours to the partons. The above-mentioned $SU(3)$ colour rules are applied only on the uncorrelated partons. The assumption of uncorrelated partons, and assigning them $SU(3)$ weighted colour compositions allows us to have an approximation of the colour configuration the partons may have. Once all the partons are assigned colours (one colour for a quark, and two colour indices for a gluon), the colour reconnection is performed based on the fundamental idea of minimising the so-called λ -measure [25]. The λ -measure gives an estimate of the number of hadrons produced in the string breakup.

Three different initial colour topologies and respectively allowed reconnections are shown in figure 2, for the colour dipoles between a quark and an anti-quark. There is one more configuration for dipoles with a long gluon chain, which are colour reconnected as *zipper-style* junctions, but we are not going into details about such complex configurations here.

For two colour dipoles, there are two possible reconnection topologies:

- (a) Ordinary style (Colour dipole swing): In this case, both dipoles exchange their colour connected partons. The QCD colour algebra will control the reconnection probability in addition to the λ measure for the new configuration. In this particular case, the reconnection probability from the QCD constraints is 1/9, since both dipoles have to have the same colour configuration.
- (b) Junction style: Instead of the reconnection of the dipole endpoints, a new string piece is created connecting the two quarks to one end of the string piece, and two anti-quarks to the other end. This configuration creates a junction and an anti-junction connected by a string piece. The QCD probability is here 1/3, which is higher than in the previous case. However,

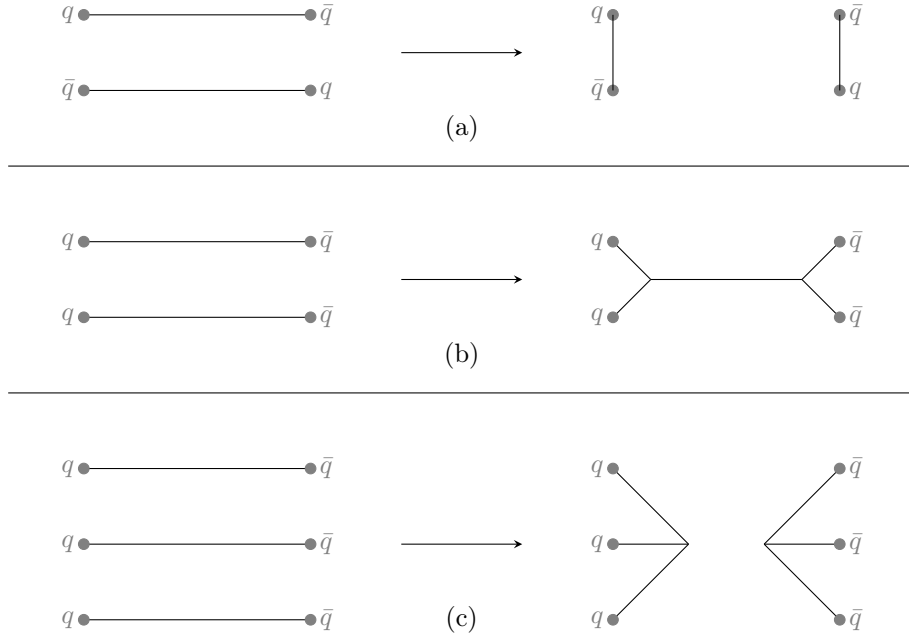


Fig. 2: Two dipoles and three dipoles CR possibilities. For two dipoles, they can either have (a) a simple reconnection (a.k.a. a *swing*) or (b) a formation of a connected junction and anti-junction system. Three dipoles can form (c) disconnected junction and anti-junction systems.

the potential reduction in the λ -measure in this type of configuration is smaller, due to the creation of a new string piece. Hence, the algorithm suppresses such a configuration.

The QCD-CR model has also a possibility for reconnection for three colour dipoles:

- (c) Junction style (Three dipoles): Two independent string systems with a junction and an anti-junction are formed after the reconnection. In this case, the QCD probability is $1/27$.

Similarly, colour reconnections are performed for dipoles containing $q - g$, $g - g$, and $\bar{q} - g$. For all types of colour dipoles, the reconnection probability is controlled by the $SU(3)$ colour algebra and the λ -measure.

In the model implementation, some simplifications are made. All dipoles are assigned colour indices from 1 to 9. For the ordinary swing reconnection to be allowed, two dipoles have to have the same index, which will provide a $1/9$ probability. For the case of junction style reconnection between two dipoles, the constraint is that the dipole indices have to be different but their value

modulo three has to be the same, giving the probability $2/9$. Similarly, for the three dipoles case the junction style CR will require all three dipoles to have different indices, but the same value for the modulo three of the dipole indices, giving the probability $2/81$.

Clearly the junction formation reconnections are here suppressed compared to the pure colour algebra ($1/3 \rightarrow 2/9$ and $1/27 \rightarrow 2/81$ respectively), and to compensate for this a special parameter C_j is used to decrease the λ -measure for junction systems in the model to favour junction formation over the swing reconnection.

The above constraints will only decide if a certain colour configuration will be allowed or not. To determine if the allowed configuration is preferred or not, the model calculates the λ -measure. The model only allows the reconnection between the two or three dipoles if the λ -measure of the new configuration is lower than the original one.

2.1 Spatially constrained model

In the QCD-CR model, all colour dipoles are allowed to undergo CR in pp collisions in PYTHIA. For any two (or three) dipoles, whether they will

be colour reconnected or not, is primarily decided based on whether the colour indices match and whether or not the colour reconnection will reduce the overall λ -measure.

Our aim is to treat super-positioned pp like events as a single HI event as early as possible in the Angantyr model. One way is to perform CR on all the colour dipoles from all the sub-collisions before the hadronization stage in the Angantyr model. But the spatial span of a HI collision can be as large as the diameters of the two colliding nuclei. The strong force is a short range force, and its range is approximately the size of a proton. Therefore, it is essential to introduce an additional spatial constraint between the colour dipoles to be colour reconnected.

The primary assumption in this work is that the majority of the colour dipoles are more or less parallel to the beam axis, and they are separated in the transverse plane. Hence we use the transverse positions of the partons to determine the separation between any two colour dipoles. For a more realistic constraint, one must take into account the full 3+1-dimensional space-time coordinates. Here we instead make a simplified assumption that the position of the dipole in the impact parameter can be represented by the midpoint between the two partons. If the distance between two such dipole's midpoints is larger than some parameter, δb_c , they should not be allowed to reconnect.

When we apply the spatial constraint in the QCD-CR model in pp collisions, the direct consequence of the constraint will be on the multiplicity distribution: fewer dipoles are now allowed to undergo CR compared to the default setup, the total multiplicity distribution will increase. But also other observables will be affected, such as $\langle p_\perp \rangle (N_{ch})$ and the p_\perp distribution. Before applying the spatial constraint to HI collisions, we will therefore need to re-tune some of the parameters of the MPI and QCD-CR models to retain a good description of pp data.

In HI collisions, the spatial constraint will allow CR among the nearby colour dipoles independent of their original sub-collisions. This will increase CR in a HI event, especially in *central* collisions, and thus reduce the multiplicity. To counteract this we will need to retune some of the parameters in the Angantyr model.

In section 3, we will discuss the selection of the parameters we will retune and examine how they affect relevant observables.

2.2 Improved junction handling

Compared to the default reconnection model in PYTHIA8, the QCD-CR results in an increase in simulation time. This could be expected due to the increase in complexity of the algorithm. We noticed, however, that the primary cause of the increase was the high failure rate in the hadronization of the junction systems. Many junction systems do not hadronize properly at the first attempt, and the algorithm has to repeat the process multiple times to succeed.

Moreover, when running the QCD-CR for HI collisions we noticed that a substantial number of events were thrown away because PYTHIA8 was not able to hadronize certain complicated junction systems. Normally such errors are unimportant, but since these errors were more frequent in high multiplicity events, they caused an artificial skewing of the overall multiplicity distribution. This is noticeable already in pp and became quite significant in AA. For this reason, we decided to improve the handling of the junction hadronization in PYTHIA8. The changes we made are mainly technical improvements and will be included in a future PYTHIA8 release. For completeness, we include the details of these changes in appendix A.

The direct consequence of our modifications in the junction hadronization can be seen in pp collisions as an enhancement of high multiplicity events. In figure 3 we show example multiplicity distributions in CMS and ATLAS minimum bias events, compared to the result from the QCD-CR(mode-0) predictions and the results of our modifications (labelled SC-CR for *Spatially Constrained* CR), but with an allowed dipole separation so large that only the effects of the modified junction hadronization are included. In the left-most figure, we show two values of the allowed dipoles separation, $\delta b_c = 1$ and 5 fm, to show that already 1 fm is large enough to remove the effect of the spatial constraints.

Clearly, the QCD-CR needs to be returned when introducing the improved junction hadronization, but in the following, we will also

want to tune the value of the allowed dipole separation in light of using the SC-CR model also for heavy ion collisions.

3 Selection of parameters and retuning strategy

There are many parameters within and outside the QCD-CR model, which can be re-tuned. Table 1 shows the set of the parameters re-tuned when the QCD-CR model is introduced in PYTHIA.

The parameters in the first part of Table 1 are tuned outside of the QCD-CR model. Those parameters directly affect the flavour production under string breaking during the fragmentation stage in the hadronization framework. The primary reason for re-tuning those parameters was to adjust the flavour production under the new colour reconnection treatment. We decided not to modify the parameters associated with the string breaking and quark-antiquark pair creation with the parameters in this analysis, and instead mainly focus on the parameters governing the overall multiplicity.

We selected the following parameters to retune against pp data:

1. $p_{\perp 0}^{\text{ref}}$, low- p_{\perp} suppression for MPIs,
2. m_0 , a scale parameter used in the λ -measure and a mass cut-off for pseudo-particles (see section 3.2),
3. C_j , a parameter reducing the λ -measure for junction systems,
4. δb_c , the allowed dipole separation.

The last one of these is the new parameter we introduce in PYTHIA¹ which gives maximum transverse distance between centres of a dipole pair to be considered for reconnection (in femtometres). δb_c also restricts the junction formation with three dipoles. If any of the three dipole pairs is separated with a transverse distance larger than δb_c , then those three dipoles are not allowed to form junctions.

The primary strategy for our retuning is to first modify these four parameters, and after an acceptable tune for pp observables has been obtained we turn to pA and try to adjust parameters

in the Angantyr model to also get an acceptable description there. The main feature of the Angantyr model affecting the overall behaviour of the multiplicity is the treatment of secondary non-diffractive (SND) sub-collisions.

The SND interactions are introduced in the Angantyr model to treat situations, where a nucleon is tagged as a participant in multiple non-diffractive type collisions with other nucleons. While primary collisions are generated as normal non-diffractive pp events, these secondary ones are generated as a diffractive excitation of the additional nucleon. This is the main feature that allows Angantyr to reproduce general features of the final state multiplicity in pA and AA events. In [6] we modified the Pomeron parton distribution functions (PDFs) for SND events. In this work, we have decided to rather modify the Pomeron flux in SND events, and modify the so-called ϵ_{pom} parameter. Modification of this parameter is aimed to modify only the SND interactions. Since SND interactions do not occur in pp collisions, we can not tune the ϵ_{pom} parameter there.

After obtaining a reasonable fit to pA data, we can use the obtained tune to generate AA events, and at this stage, there are no further parameters to tune.

In the following we will study the effects of the selected parameters individually. We will restrict our study to typical minimum bias observables such as charged multiplicity distributions and $\langle p_{\perp} \rangle (N_{ch})$.

3.1 Low- p_{\perp} suppression for MPIs

For minimum bias events, PYTHIA regularise the QCD $2 \rightarrow 2$ process by introducing a collision energy dependent parameter $p_{\perp 0}$ to regularise the divergences in the partonic cross section

$$\frac{d\sigma_{2 \rightarrow 2}}{dp_{\perp}^2} \rightarrow \frac{d\sigma_{2 \rightarrow 2}}{dp_{\perp}^2} \times \frac{p_{\perp}^4}{(p_{\perp}^2 + p_{\perp 0}^2)^2} \frac{\alpha_s^2(p_{\perp}^2 + p_{\perp 0}^2)}{\alpha_s^2(p_{\perp}^2)} \quad (1)$$

Here α_s is the strong coupling constant, and p_{\perp} is the transverse momentum of the scattered partons. The energy dependence of the parameter $p_{\perp 0}$ is further given by another parameter $p_{\perp 0}^{\text{ref}}$. The power law dependent relation is given as

$$p_{\perp 0} = p_{\perp 0}(E_{\text{cm}}) = p_{\perp 0}^{\text{ref}} \times \left(\frac{E_{\text{cm}}}{E_{\text{cm}}^{\text{ref}}} \right)^{p_{E_{\text{cm}}}}, \quad (2)$$

¹In PYTHIA this parameter is now called `ColourReconnection:dipoleMaxDist`.

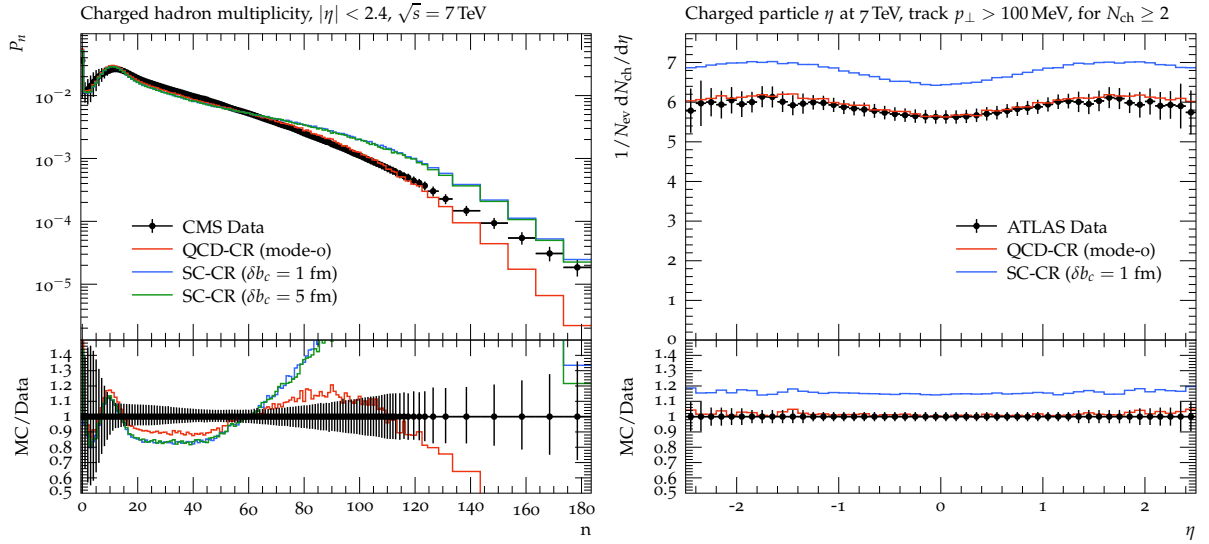


Fig. 3: The effect of improved junction hadronization in PYTHIA8 before retuning. Events are generated for $\sqrt{s} = 7$ TeV pp non-single-diffractive collisions and compared with CMS [26] and minimum bias collisions with ATLAS [27] data. *Left:* multiplicity in $|\eta| < 2.4$ with CMS data. *Right:* multiplicity distribution in η for $|\eta| < 2.4$ with ATLAS data. The red line shows the results for default QCD-CR (Mode-0) in PYTHIA8, and the blue and green lines represent the results for SC-CR with improved junction hadronization and added spatial constraint set to large values: blue lines $\delta b_c = 1$ tm and green line $\delta b_c = 5$ fm.

Parameters	Monash	QCD-CR (Mode-0)
StringPT:sigma	0.335	0.335
StringZ:aLund	0.68	0.36
StringZ:bLund	0.98	0.56
StringFlav:probQQtoQ	0.081	0.078
StringFlav:ProbStoUD	0.217	0.2
StringFlav:probQQ1toQQ0join	0.5, 0.7, 0.9, 1.0	0.0275,0.0275,0.0275,0.0275
BeamRemnants:remnantMode	0	1
BeamRemnants:saturation	-	5
MultiPartonInteractions:pT0Ref ($p_{\perp 0}^{\text{ref}}$)	2.28	2.12
ColourReconnection:mode	0	1
ColourReconnection:allowDoubleJunRem	-	off
ColourReconnection:m0 (m_0)	-	2.9
ColourReconnection:allowJunctions	-	on
ColourReconnection:junctionCorrection (C_j)	-	1.43
ColourReconnection:timeDilationMode	-	0

Table 1: The list of parameters and their values in the Monash tune, and in the QCD-CR (Mode-0) tune in PYTHIA8.

where $p_{E_{\text{cm}}}$ is a scaling parameter, controlling the growth of $p_{\perp 0}$ with the centre of mass energy of the collision, E_{cm} , with respect to a reference energy, $E_{\text{cm}}^{\text{ref}}$, which by default is set to 7 TeV in PYTHIA.

The effects of varying $p_{\perp 0}^{\text{ref}}$ on the event multiplicity and $\langle p_{\perp} \rangle(N_{ch})$ distribution is shown in Figure 4. Here (and also in Figures 6 and 7 below) we compare result for default PYTHIA8 with the

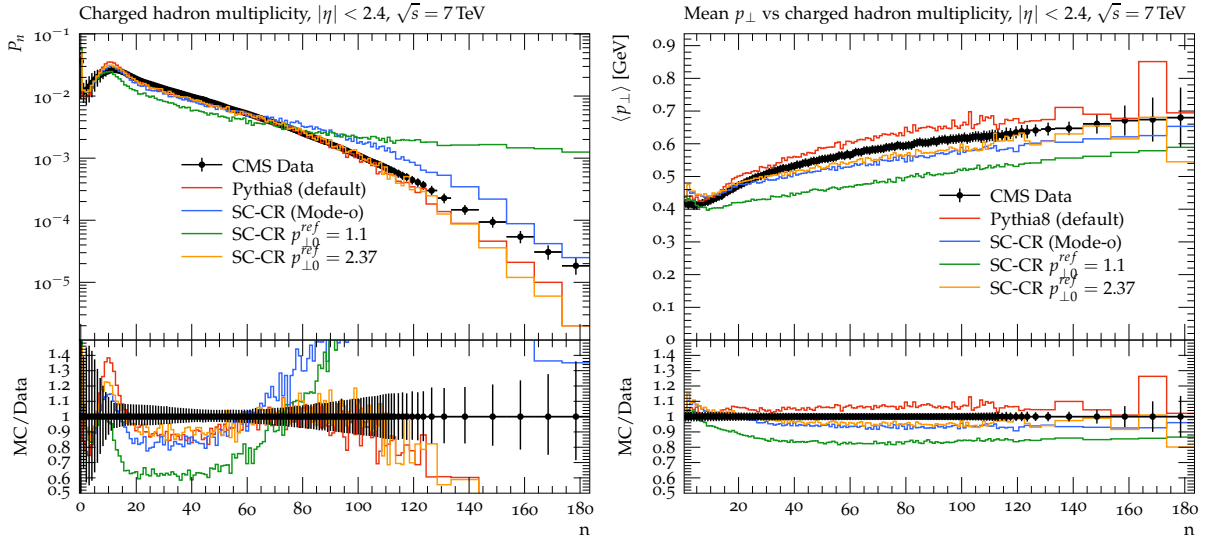


Fig. 4: The effect of varying the $p_{\perp 0}^{\text{ref}}$ parameter in PYTHIA8. Events are generated for $\sqrt{s} = 7$ TeV pp non-single-diffractive collisions and compared with CMS data [26]. *Left:* multiplicity in $|\eta| < 2.4$. *Right:* $\langle p_{\perp} \rangle$ vs N_{ch} for $|\eta| < 2.4$. The red line shows the results for default PYTHIA8, the blue line the results for SC-CR (Mode-0), while the green and orange lines show the effects of varying $p_{\perp 0}^{\text{ref}}$ in the latter.

results for the SC-CR (with all parameters set as in Mode-0 in Table 1 and with $\delta b_c = 1$ fm). The main effect of reducing $p_{\perp 0}^{\text{ref}}$ is an increase of multiple scatterings which increases the multiplicity and reduces the average transverse momenta, which is indeed what is shown in the figure.

3.2 m_0 and C_j parameters

The parameter m_0 is the mass scale in the λ -measure [25] used in the QCD-CR model. C_j is a parameter which modifies this mass scale in string pieces connected to a junction, according to $m_{0j} = C_j m_0$.

In the QCD-CR model, there is a special treatment of small-mass string pieces. Any dipole with invariant mass less than the m_0 scale will not be allowed to reconnect but is instead collapsed into a pseudo-particle.

Figure 5 shows how one short dipole or two short dipoles are replaced by a *pseudo-particle* in a normal dipole chain (top panel), and in a junction system (bottom panel). The invariant mass of every dipole is compared with m_0 , and if it's smaller than m_0 then the dipole is replaced with a *pseudo-particle*, which has the four-momentum of the dipole. Dipoles on both ends of the short dipole are connected to the *pseudo-particle*. This

way the value of m_0 will directly control the number of dipoles that undergoes CR in the QCD-CR model. These small dipoles are only removed during the CR, but they do contribute to the hadron production. Therefore the parameter m_0 significantly affects the hadron multiplicity in the event final state. The removal of *small* dipoles is due to technical reasons, and to reduce the complexity of the CR process [17]. It is suggested that in the QCD-CR [17] model the parameter m_0 having its value around Λ_{QCD} has negligible effect, but raising its value beyond 1 GeV significantly reduces the amount of the colour reconnection.

The λ -measure used in [25] is an infrared safe measure of partonic final states, approximately proportional to the resulting hadronic multiplicity. In the QCD-CR, an approximation is used, which is good for large energies. For string pieces between gluons and/or massless quarks, it is given by

$$\lambda = \ln \left(1 + \frac{\sqrt{2}E_1}{m_0} \right) + \ln \left(1 + \frac{\sqrt{2}E_2}{m_0} \right), \quad (3)$$

where energies are calculated in the dipole's rest frame. In the parentheses, 1 is added to avoid negative contributions.

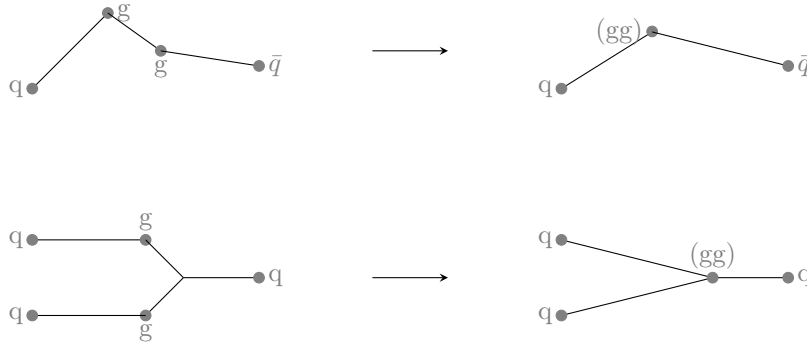


Fig. 5: Top) Pseudo-particle is formed from a dipole that has a smaller invariant mass than m_0 in a string, and Bottom) Pseudo-particles are formed if the dipole is connected to a junction.

In the current QCD-CR implementation in PYTHIA8, the value for *pseudo-particle* mass cut-off is also used in the calculation of the λ -measure. But in principle, one could treat them as independent parameters.

Eq. (3) is also used for a string piece connected to a junction, where the energy is measured in the junction rest frame. For a string piece connecting two junctions the λ -measure is given by [28]. The distance between the two junctions is also added to the calculation of the λ -measure of the new system and is given by

$$\lambda = \log \left(\beta_{j1}\beta_{j2} + \sqrt{(\beta_{j1}\beta_{j2})^2 - 1} \right), \quad (4)$$

where β_{j1} and β_{j2} are 4-velocities of the two junctions.

The parameter m_{0j} is used in the λ -measure calculation for the junction systems, while the m_0 is used for the λ -measure of the dipoles. Increasing m_{0j} results in a lower value for the λ -measure, which favours junction production. In this way the suppression of junctions in the model compared to proper $SU(3)$ algebra can be compensated by using a value above unity for the parameter C_j .

Figure 6 shows the effect of varying m_0 on the final state charged multiplicity and $\langle p_\perp \rangle(N_{ch})$ compared with CMS data for $\sqrt{s} = 7$ TeV pp NSD collisions. It is evident that increasing m_0 increases the event multiplicity, by reducing the number of dipoles in CR, and vice versa.

Figure 7 shows the effect of varying C_j on the final state charged multiplicity and $\langle p_\perp \rangle(N_{ch})$ compared with CMS data for $\sqrt{s} = 7$ TeV pp

NSD collisions. The histograms show that reducing C_j below 1 increases the multiplicity because it reduces the number of junctions, which allows the production of many light hadrons. But enhancing its value will not have any significant effect on the observables. It is also evident from the histograms that varying m_0 has relatively strong effects on the observables compared to varying C_j .

3.3 Allowed dipole separation

The parameter δb_c constrains colour reconnection between the colour dipoles by constraining the transverse separation. We now fix all the parameters to QCD-CR (mode-0) and vary the δb_c . The effect on the event multiplicity and $\langle p_\perp \rangle(N_{ch})$ due to varying δb_c between two and three dipoles to be colour reconnected is shown in Figure 8, and it is compared with CMS data for $\sqrt{s} = 7$ TeV pp NSD collisions. From the figure, we see that reducing δb_c as low as 0.3 fm will reduce the CR significantly, increase the charged multiplicity and make the $\langle p_\perp \rangle(N_{ch})$ distribution flatter.

In a nutshell, each of the parameters discussed above has their contribution to the total charged multiplicity, which is summarised in table 2. The direction of the arrows in the bracket next to every parameter shows the direction in which the histogram lines will move with respect to the earlier value of the parameter if all the other parameters are fixed.

3.4 ϵ_{pom} for SND events

The default Angantyr simulates SND events using a proton-like pomeron PDF, a pomeron-proton

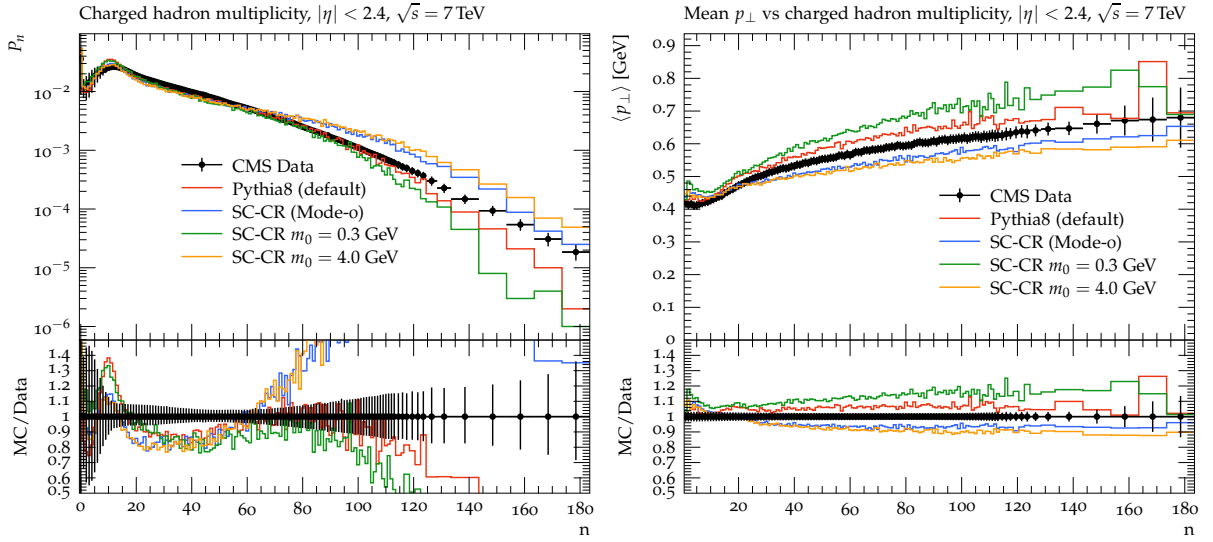


Fig. 6: The same as Figure 4, but here the green and orange lines show the effect of varying the m_0 parameter in the SC-CR model.

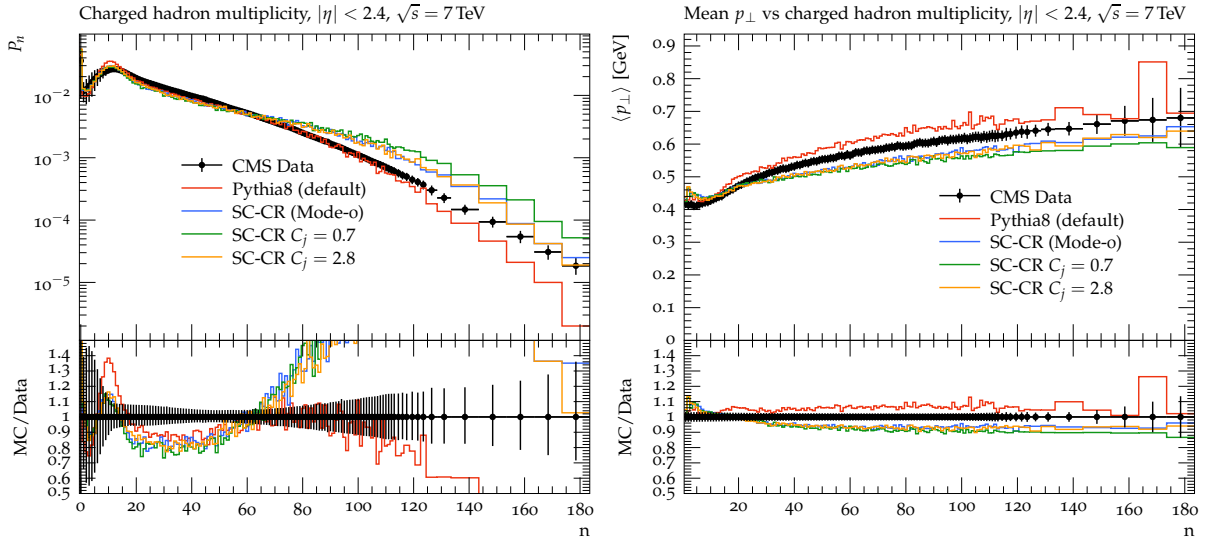


Fig. 7: The same as Figure 4, but here the green and orange lines show the effect of varying the C_j parameter in the SC-CR model.

interaction cross-section similar to the proton-proton non-diffractive interaction cross-section, and the pomeron flux according to Schuler and Sjöstrand [29], which gives a logarithmic distribution in the mass of the diffracted system, dm^2/m^2 .

When we now introduce CR also between different sub collisions in a HI event we expect the

overall multiplicity to go down, possibly destroying the good reproduction of data reported in [6]. To compensate for this we want to modify the pomeron flux in the SND events, and we use a conventional supercritical description for the pomeron flux, attributed to Berger *et al.* [30] and Streng [31]. The Pomeron Regge trajectory is

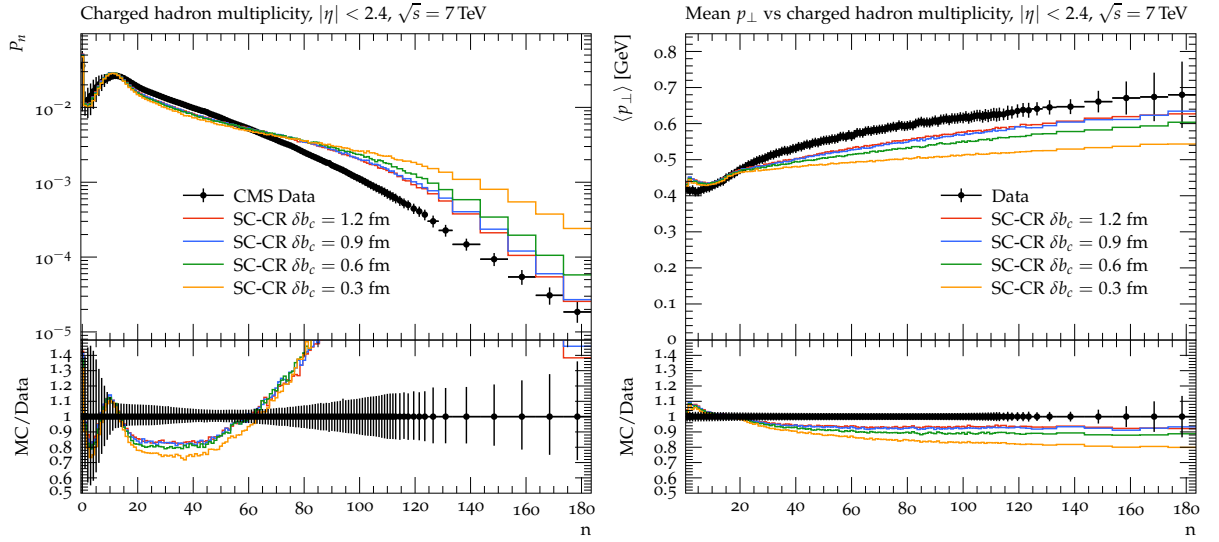


Fig. 8: Comparing variation in the δb_c parameter in PYTHIA8. Events are generated for $\sqrt{s} = 7$ TeV pp NSD collisions and compared with CMS data [26]. *Left:* charged hadron multiplicity in $|\eta| < 2.4$. *Right:* $\langle p_\perp \rangle$ vs N_{ch} for $|\eta| < 2.4$.

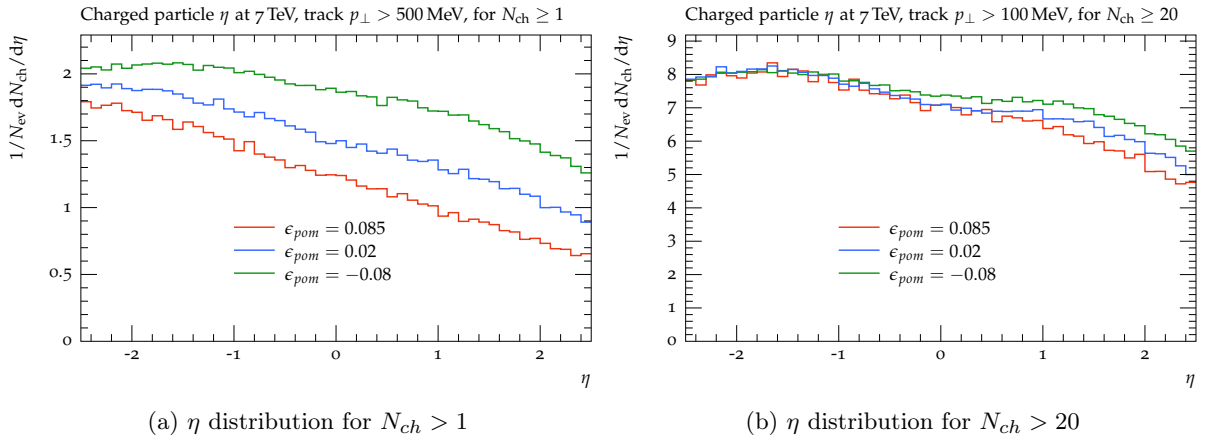


Fig. 9: Angantyr SND events, which are single diffractive (SD) events generated for $\sqrt{s} = 7$ TeV pp collisions, with `HeavyIon:Mode = 2`, and `Angantyr:SDTests = on` in PYTHIA8. Here the SD events are generated in the `Angantyr:SASDmode = 4`. Changing ϵ_{pom} from positive to negative values, the event multiplicity increases, and the overall distribution is a bit flatter, but closer to the diffractive proton side (negative η), its similar to ND as expected.

parameterized as:

$$\alpha(t) = 1 + \epsilon_{pom} + \alpha'(t), \quad (5)$$

giving the mass distribution $dm^2/m^{2(1+\alpha(t))}$. We can then vary ϵ_{pom} , which is a parameter to

modify the mass distribution in the diffracted system.

The effect of changing the ϵ_{pom} parameter for the low and high multiplicity SND events in Angantyr is shown in Figure 9. As expected we see an increase in the multiplicity when changing ϵ_{pom} from positive to negative values.

Parameters	Charged Multiplicity
$p_{10}^{\text{ref}} (\downarrow)$	\uparrow
$m_0 (\downarrow)$	\downarrow
$C_j (\downarrow)$	\uparrow
$\delta b_c (\downarrow)$	\uparrow

Table 2: A list of parameters and the effects on the overall multiplicity in PYTHIA8. When the parameter is reduced (\downarrow) the overall multiplicity will increase (\uparrow) or decrease (\downarrow), when keeping all other parameters fixed.

It should be noted that the default value of ϵ_{pom} in PYTHIA8 is 0.085, which gives a good fit for diffractive events in pp. However, when we here use this to generate SND events, we do not expect them to behave exactly like diffractive events. In [6] we discussed the relationship between the SND in double nucleon scattering and single diffraction (see the discussion of Figure 22) and argued that the mass distribution should not be the same in the two cases. The mass distribution in single diffraction is related to the rapidity span of the diffracted system, $dm^2/m^2 \approx d\Delta y_m$, while in the SND we expect it to be proportional to the rapidity gap, $dm^2/m^2 \approx d\Delta y_{gap}$, single diffraction, with $\Delta y_{gap} = \Delta Y - \Delta y_m$, where ΔY is total rapidity span of the pp collision. Therefore, if a positive ϵ_{pom} is needed to describe single diffraction, using a negative value is quite reasonable for the SND, which is what we need in order to compensate for the decrease in multiplicity due to the CR in HI collision.

3.5 CR effects in pA and AA collisions

This is the first time that the effects of CR have been introduced and studied in a heavy-ion collision event-generator. In section 2, we show the importance of the CR in the context of e^+e^- and pp collision event simulations in PYTHIA. In this work, we are further extending the Angantyr model of PYTHIA8 with a global CR, which is constrained by the transverse separation of the colour dipoles. For the sake of completeness, it is interesting to see how large the effects of colour reconnections really are before retuning. We have looked at pPb and PbPb central charged event multiplicities for the default Angantyr setup, where there are colour reconnections only inside

individual NN sub-collisions. This we then compared to the case where reconnections are switched off altogether, and to the case where we have global reconnections between (almost) all dipoles in the event. We have used the QCD-CR (mode-0) parameters for the latter, but the δb_c value is set to 7 fm.

The results are shown in Figure 10, where it is clear that the effects of colour reconnections are substantial mainly for the highest multiplicities. The average multiplicities are however only moderately affected, with a 20% increase for PbPb when reconnections are switched off, and a 10% decrease with global reconnections. The corresponding effects in pPb are smaller, with +10% and -5% respectively.

4 Results

First, we note that we have not done a very sophisticated retuning of the parameters, *e.g.*, using the Professor framework [32]. Our focus has been to get a reasonable multiplicity distribution for pp and also for pA. There is some tension in data, favouring a larger δb_c in pp, but a lower one in pA. In the end, we basically selected the value $\delta b_c = 0.5$ fm.

We show the tuned values under the SC-CR (tuned) column and the default values of those parameters under the QCD-CR (mode-0) column in Table 3. For pp, all other parameters are the same as for QCD-CR (mode-0), which is shown in Table 1.

To treat a heavy-ion event as a single event we want to stack all pp-like sub-collisions at the parton level, and then apply CR with spatial constraints on all colour dipoles. To do so, we first turn off colour reconnection in all individual sub-collisions (`ColourReconnection:reconnect = off`) and instead switch it on only for the hadronization stage (`ColourReconnection:forceHadronLevelCR = on`).²

Now, with this feature enabled, pA and AA collision events undergo CR only once per HI event, and after CR the entire event proceeds

²At the moment this combination works only within the Angantyr framework. Moreover, it does not work with PYTHIA's default MPI-based CR. For pp collisions, this feature is not that useful, as there's only one proton-proton collision which is a single event by default. But if a user wishes, one can use the above combination for pp collisions as well by setting the `Heavyion:mode = 2` flag to generate pp collisions within the Angantyr setup.

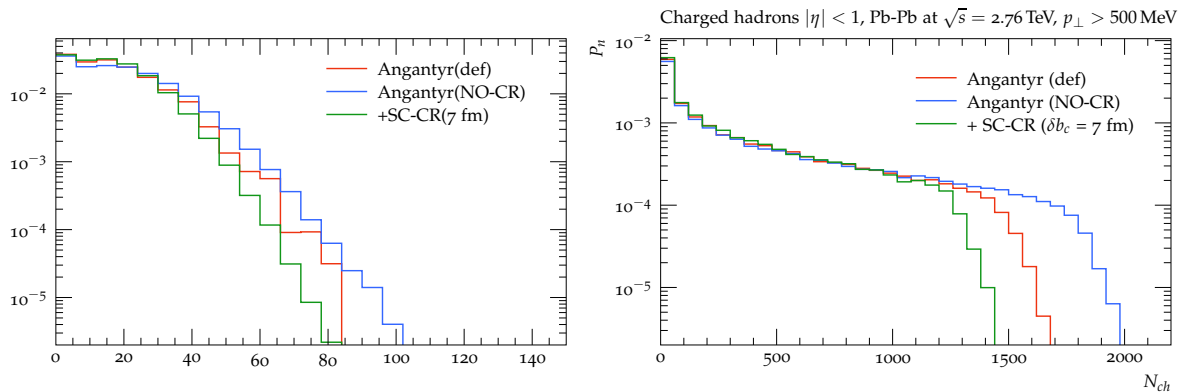


Fig. 10: The distribution in charged hadrons multiplicity in $|\eta| < 1$ and with $p_{\perp} > 500 \text{ MeV}$ for pPb events at $\sqrt{s_{NN}} = 5.02 \text{ TeV}$ (left) PbPb events at $\sqrt{s_{NN}} = 2.76 \text{ TeV}$ (right). The red lines are for the events generated with the default Angantyr. The blue lines are the events with no CR reconnection between the colour dipoles, and the green lines are the events generated with QCD-CR (mode-0) parameters, but the δb_c value is set to 7 fm, which is almost the radius of a Pb nucleus.

Parameters	QCD-CR (Mode-0)	SC-CR (tuned)
PartonVertex:setVetex	-	on
MultiPartonInteractions:pT0Ref	2.12	2.37
ColourReconnection:m0	2.9	1.05
ColourReconnection:junctionCorrection	1.43	1.37
ColourReconnection:dipMaxDist	-	0.5

Table 3: The list of parameters and their new values compared to their values in the QCD-CR (Mode-0) tune. The new values are used in PYTHIA8 to generate pp collisions with the spatial constraint in the SC-CR model.

to hadronization. The list of changed and new parameters for HI collisions is shown in Table 4. The prefix "HI" for some of the parameters means that they are only used for SND sub-collisions.

4.1 pp results

We begin with comparing pp events generated at $\sqrt{s} = 7 \text{ TeV}$ using PYTHIA8 default and re-tuned spatially constrained QCD-CR in PYTHIA8. We show the charged multiplicity and $\langle p_{\perp} \rangle(N_{ch})$ distributions for these two setups and compare the results with ATLAS [27] and CMS [26, 33] experiments. The pp results compared with ATLAS are minimum bias events, while the events compared with the CMS experiment are generated as non-single diffractive (NSD) events in PYTHIA8. We use $c\tau > 10 \text{ mm}$ as the definition for primary particles when comparing our simulated events against ATLAS and CMS data.

In figure 11 we show that with the new constraint on QCD-CR and the new tuned parameters, we are able to reasonably reproduce the average event multiplicity and $\langle p_{\perp} \rangle(N_{ch})$ distributions from the ATLAS and CMS for $\sqrt{s} = 7 \text{ TeV}$ pp collisions. This should not be surprising, since these are the distributions we tuned to.

Figure 12 shows the distribution in p_t and N_{ch} compared to ATLAS data, and here we observe that the charged multiplicity distribution for the SC-CR setup drops too quickly for high multiplicities. We also see that the transverse momentum spectrum becomes too hard. These effects are related: when we introduce the spatial constraint, there will be less reconnection and thus higher multiplicity; this is then compensated somewhat by decreasing m_0 , but this is not enough (remember that QCD-CR (mode 0) also has a too high multiplicity when our improved junction handling is introduced); so we increase the $p_{\perp 0}^{\text{ref}}$ but that

Parameters	QCD-CR (Mode-0)	SC-CR (new)
ColourReconnection:reconnect	on	off
ColourReconnection:forceHadronLevelCR	off	on
MultiPartonInteractions:pT0Ref	2.12	2.37
PartonVertex:setVetex	-	on
ColourReconnection:m0	2.9	1.05
ColourReconnection:junctionCorrection	1.43	1.37
ColourReconnection:dipMaxDist	-	0.5
HIMultiPartonInteractions:pT0Ref	2.12	2.37
HISigmaDiffractive:mode	-	0
HISigmaDiffractive:PomFlux	-	3
HISigmaDiffractive:PomFluxEpsilon	-	-0.04
HIBeamRemnants:remantMode	-	1
HIBeamRemnants:Saturation	-	5
BeamRemnants:beamJunction	off	on
HIBeamRemnants:beamJunction	off	on

Table 4: The list of parameters and their new values compared to their default values in the QCD-CR (Mode-0) tune. The new values are used in the Angantyr model to generate pA and AA collisions with the spatial constraint in the SC-CR model. The values for the parameters used to generate pp events are not changed, and they are same as in Table 3, while the other parameters are same as in Table 1.

mainly decreases the multiplicity of low transverse momentum particles, giving a too hard spectrum. The conclusion is that our tuning may have been a bit naive, but for now, we are satisfied with that we have the overall multiplicity under control.

Although we in this paper are mainly concerned with general multiplicities and transverse momentum distributions, it is interesting to also look at other effects of the QCD-CR model. In particular the junction reconnections are interesting, as they are known to substantially affect the baryon-to-meson ratios.

Figures 13 and 14 show baryon-to-meson ratios for non-strange and strange baryons for the pp collision at $\sqrt{s} = 7$ TeV and compared with ALICE [34] results. The events are generated with default PYTHIA8 set-up and for the spatially constrained QCD CR model. The ratios of p/π , Λ/π , Λ/K_s^0 , Ξ/π , and Ω/π are produced for the combined yield of particles and respective anti-particles. We observe that the baryons production is enhanced, which is an expected outcome of using the QCD CR model [17]. From the p/π ratio plots in figure 13, we notice that the model produces too many protons, while the model improves the distribution of Λ , Ξ , and Ω baryons. We note that in pp the spatial constraint is not very important for these ratios, and similar results are expected

for the standard QCD-CR model without our modifications.

The results of the Λ/K_s^0 ratio are showing agreement with the ALICE data similar to the results obtained using the rope-hadronization [35] model in PYTHIA8. It is important to note that the CR model acts on the colour dipoles, while the rope-hadronization acts on the Lund strings during the string fragmentation. Hence it will be interesting to investigate if both models together can improve PYTHIA results and to what extent each of the models will influence the hadrons yield in all three collision systems. At the moment from the figures 12 and 13 the p_t distribution of the charged particles and the proton yield both are shortcomings of the spatially constrained QCD CR model.

4.2 pPb results

We show here comparisons between the Angantyr-generated average charged particles multiplicity as a function of pseudo-rapidity in different centrality bins for pPb collision events at $\sqrt{s_{NN}} = 5.02$ TeV, and experimental results from ATLAS [36]. For the SC-CR we use the parameter values we tuned to pp with the heavy-ion specific parameters listed in table 4, while the other parameters retain their

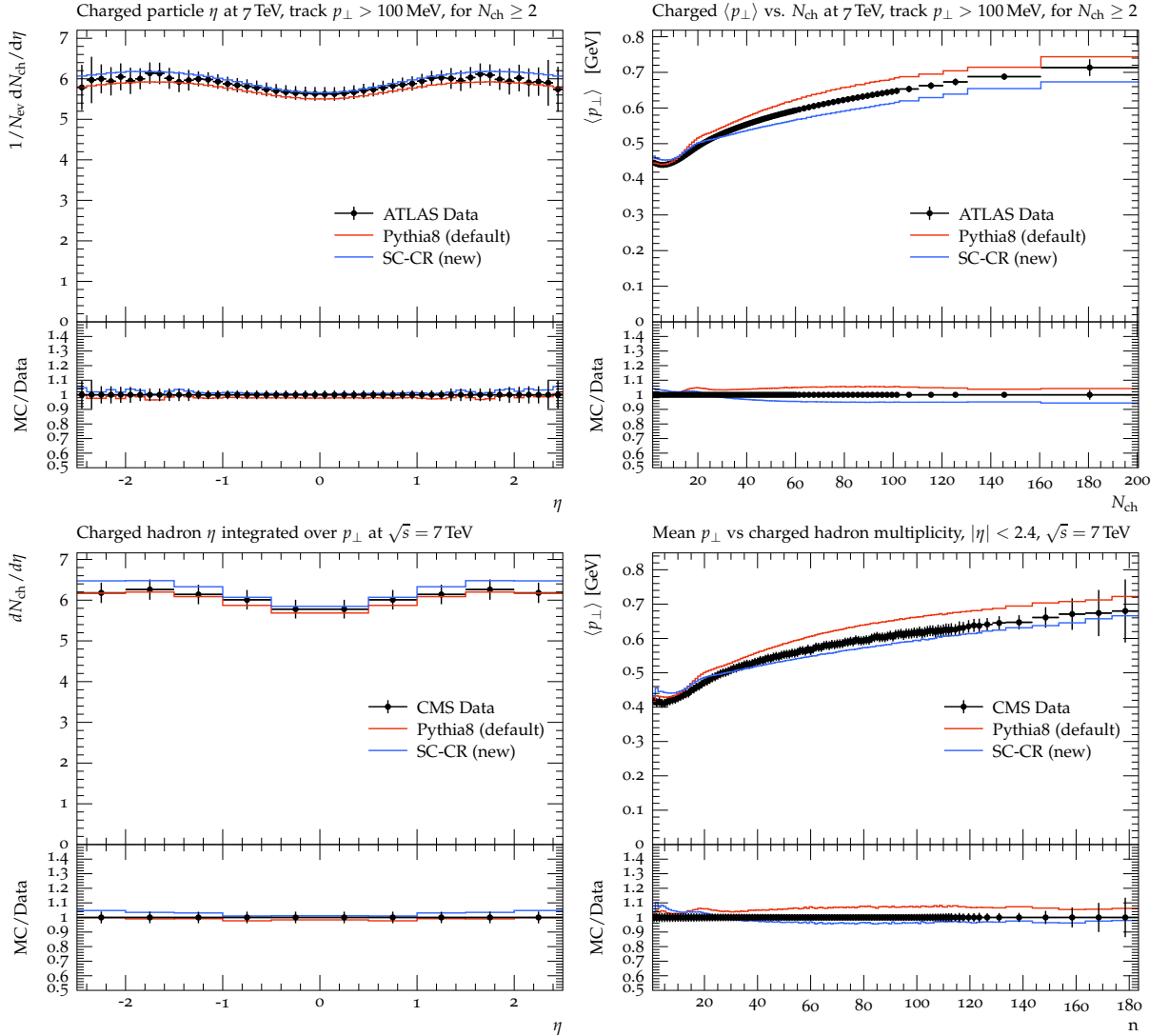


Fig. 11: Events are generated for $\sqrt{s} = 7$ TeV pp collisions minimum bias events are compared with ATLAS [27] results (top row), and non-single diffractive events are compared with CMS [26, 33] results (bottom row). The left plots show the pseudo-rapidity distribution of charged particles, while the right plots show $\langle p_{\perp} \rangle$ as a function of multiplicity. PYTHIA8 (default) is the default pp collisions with the PYTHIA8 Monash tune setup. SC-CR (new) is produced by our spatial constraint CR model, with the parameters given in Table 3.

values for QCD-CR (mode-0) in table 1. The centrality determination is made separately for each generated dataset using the standard Rivet [37] routine.³

³The centrality routine is called `ATLAS_pPb_Calib`, and the multiplicity analysis is then made with the option `cent=GEN` in Rivet.

The results are shown in Figure 15, and it is clear that just allowing for CR between individual sub-collisions (blue lines labelled “+ SC-CR ($\epsilon_{pom} = 0$)”) seriously degrades the good reproduction of data for the default Angantyr setup. This is expected as the CR necessarily will reduce the multiplicity in events with many participating nucleons. Trying to counteract this by decreasing

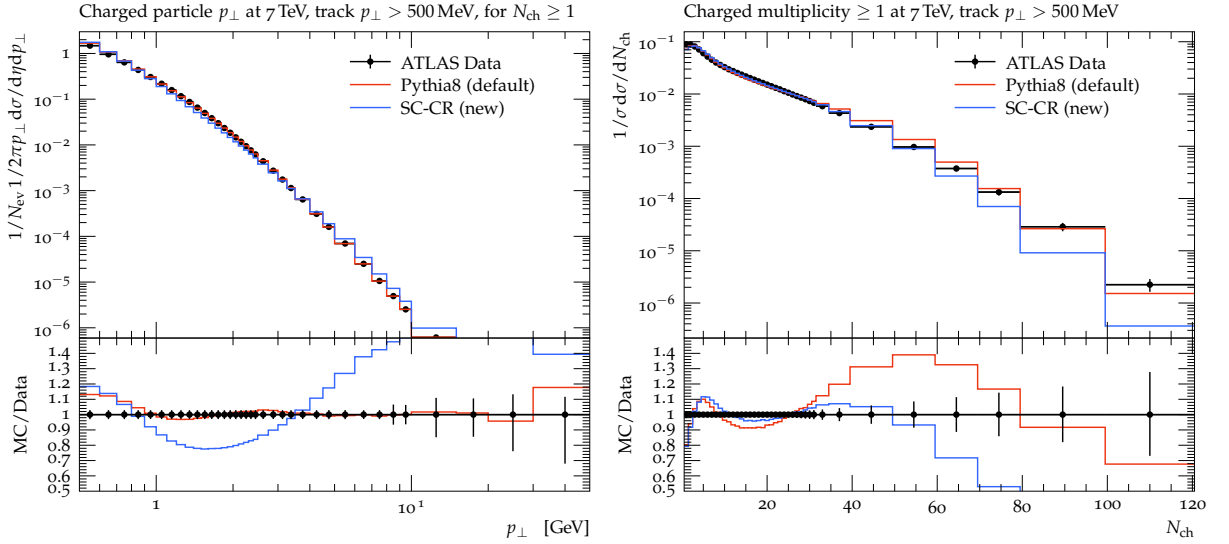


Fig. 12: Events are generated for $\sqrt{s} = 7$ TeV pp collisions minimum bias events and compared with ATLAS [27] results. The left plot shows the distribution of p_{\perp} for charged particles and the right shows the distribution in charged multiplicity. The lines are the same as in Figure 11.

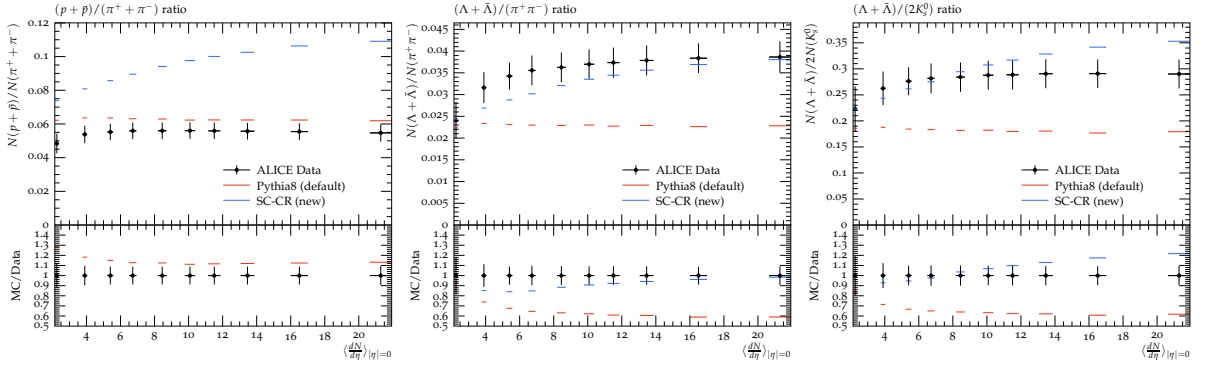


Fig. 13: From left to right the ratios of p/π , Λ/π , and Λ/K_s^0 is plotted against the average charged-particle multiplicity in the central pseudo-rapidity. pp collisions minimum bias events are generated at $\sqrt{s} = 7$ TeV and compared with ALICE [34] results. The lines are the same as in Figure 11.

ϵ_{pom} and thus increasing the multiplicity of SND sub-events, improves the reproduction of data, but as seen in Figure 15 (green lines), for the most central events it is not quite enough. We also see that for more peripheral events there is a tendency to overestimate the multiplicity, and decreasing ϵ_{pom} further to increase multiplicity in central events would also worsen the description of peripheral events.

It should be noted here that the concept of centrality in pPb, is a bit complicated, and we showed in [6] that any centrality measure will not

only be sensitive to the number of participating nucleons, but will also be sensitive to multiplicity fluctuations in individual sub-collisions, especially the most central bins. Looking back on figure 12, we see that our SC-CR tune have much fewer fluctuations to very large multiplicities than default PYTHIA in pp events, and it is possible that improving this could also help the description of very central pPb events.

Figure 16 shows the baryon-to-meson ratio for protons and Λ baryons in pPb collision events $\sqrt{s_{NN}} = 5.02$ TeV, and the results are compared

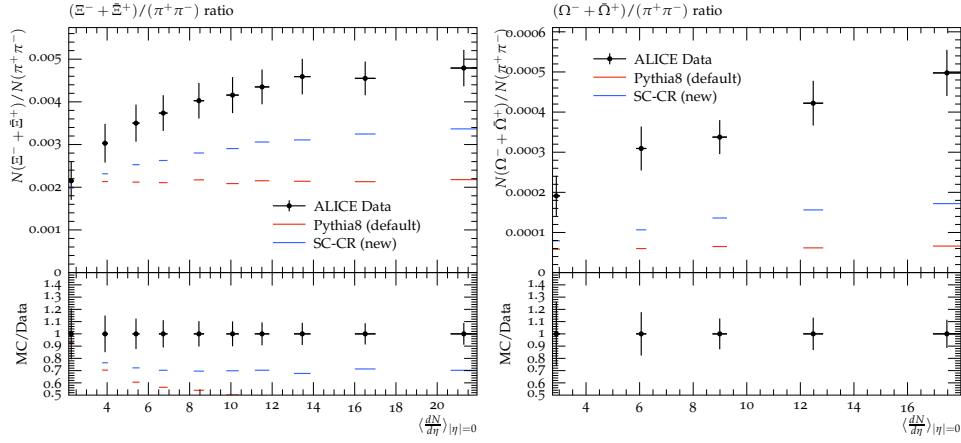


Fig. 14: From left to right the ratios of Ξ/π and Ω/π is plotted against the average charged-particle multiplicity in the central pseudo-rapidity. pp collisions minimum bias events are generated at $\sqrt{s} = 7$ TeV and compared with ALICE [34] results. The lines are the same as in Figure 11.

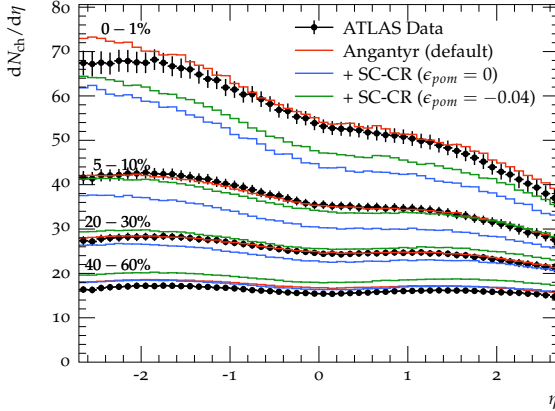


Fig. 15: Average charged hadron multiplicity as a function of η for different centrality bins for pPb events are generated at $\sqrt{s_{NN}} = 5.02$ TeV and compared with ATLAS [36] results. The red lines are Angantyr default, the blue and green ones are also from Angantyr but the blue with the spatially constrained QCD-CR (with the new tune obtained for pp collisions), and green are the same but with the tuned value of $\epsilon_{pom} = -0.04$. The top group of lines show the results from the centrality interval 0–1%, followed by the centrality intervals 5–10%, 20–30% and, at the bottom, 40–60%.

with ALICE data [38]. We can notice that the results follow the trend of baryon-to-meson ratio in Figure 13, the SC-CR model produces too many protons irrespective of the event centrality, while

the Λ/π distribution is improved compared to Angantyr (default).

4.3 PbPb results

PbPb events at $\sqrt{s_{NN}} = 2.76$ TeV were generated using the Angantyr model with its default setup and the SC-CR setup (table 4). The simulation results are compared with ALICE [39] in figure 17 (left) for the central ($|\eta| < 0.5$) charged multiplicity in different centrality bins⁴. We see here the same tendency as in pPb, that the multiplicity is reduced for central events when including CR between sub-collisions, while for more peripheral events it is less affected. The effect is roughly the same, $\sim 20\%$, for the most central events. Even though the multiplicity in PbPb is much higher, the sub-collisions are more spread out in impact parameter, and the spatial constraint, δb_c , therefore severely restricts the effect of CR.

It should be noted that the effects on the centrality binning of fluctuations in sub-collision multiplicity are not so important in PbPb, compared to pPb. This is reflected in the average number of participating nucleons as a function of centrality obtained from a Glauber model, shown in figure 17 (right). Here we see that the agreement between Angantyr, with and without SC-CR

⁴ Again the centrality bins are calculated on the generated data, this time using the ALICE_2015_PBPBCentrality analysis in Rivet

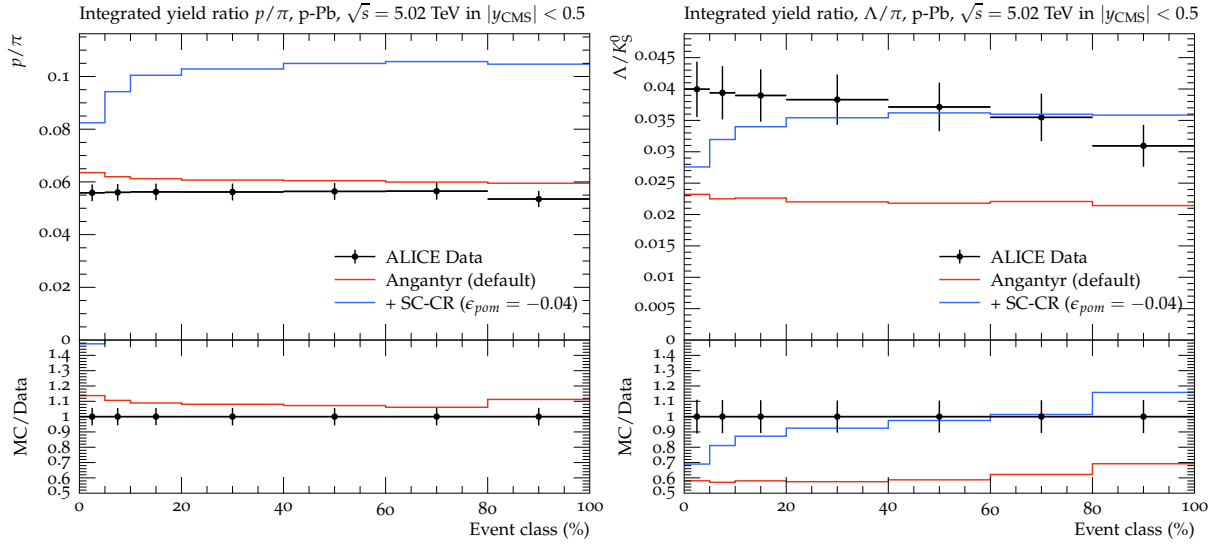


Fig. 16: The ratios of p/π (left) and Λ/π (right) are plotted for different centrality for pPb collision events at $\sqrt{s} = 5.02$ TeV and compared with ALICE [38] results. The red line is generated with the default Angantyr settings, while the blue line is SC-CR with the tune obtained for pA collisions.

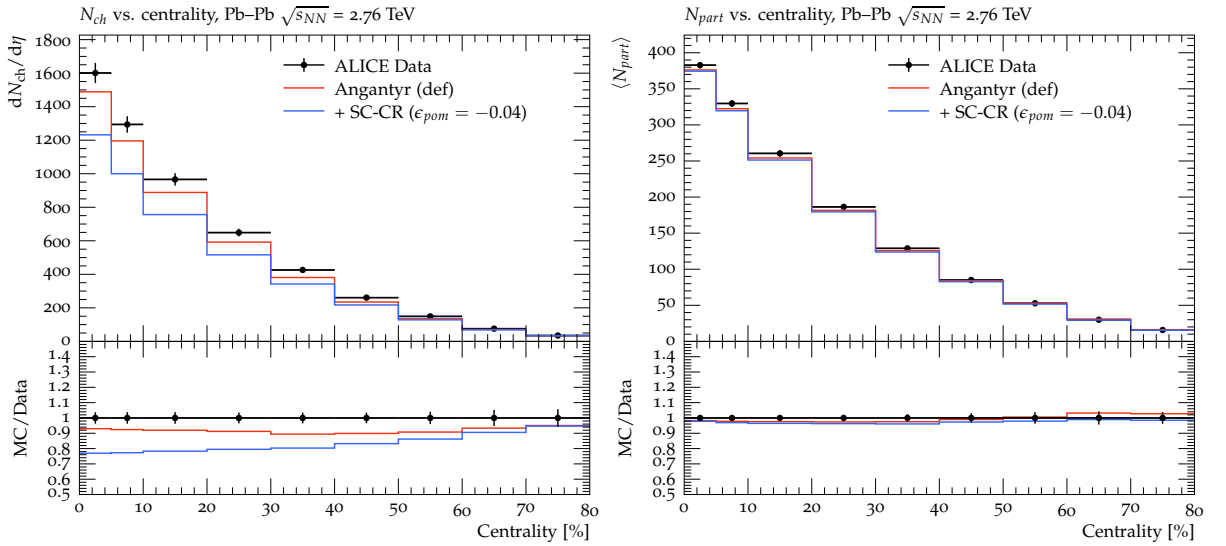


Fig. 17: *Left:* Central ($|\eta| < 0.5$) charged multiplicity as a function of centrality for PbPb collisions at $\sqrt{s_{NN}} = 2.76$ TeV. The red line is generated with the default Angantyr settings, while the blue line is SC-CR with the tune obtained for pA collisions. The data is from ALICE [39]. *Right:* number of participating nucleons, N_{part} , as a function of centrality for the same event samples, compared with Glauber-model calculations from ALICE [39].

agrees very well with each other and with the number obtained from the data.

We noted in [6] that, while the default Angantyr gives a reasonable description of the multiplicity in PbPb data, other observables were not as well reproduced. In particular this applies to p_{\perp}

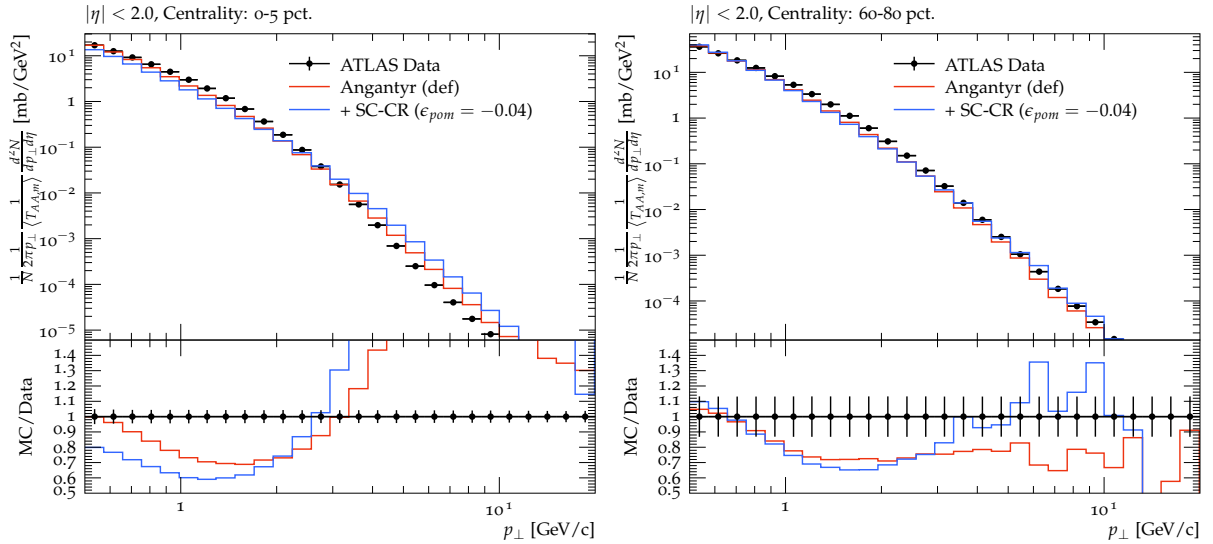


Fig. 18: Transverse momentum distribution of charged particles in different centrality bins for PbPb collisions, generated at $\sqrt{s_{NN}} = 2.76$ TeV and compared with ATLAS [40] results. The lines are the same as in figure 17.

spectra, which we show here in figure 18 compared with ATLAS [40] for central and peripheral events. Considering that we already in figure 12 showed that SC-CR degrades the description of the p_{\perp} distribution in pp, it would be unlikely that it would be better in PbPb. Indeed we see in the figure that adding global colour reconnection in PbPb, rather makes the description of data worse in central collisions. For peripheral collisions, one could argue that there is an improvement in the high- p_{\perp} tail, but the overall performance is still not very good.

So far for pp and pPb, we have shown proton-to-pion and some of the hyperons-to-pion ratios. For PbPb we want to refrain from showing any baryon-to-meson results. The SC-CR model fails to reproduce the charged multiplicity for many centrality bins in PbPb collision events. Hence the model's agreement or disagreement with the experimental data of baryon-to-meson ratios will be irrelevant at this stage. We want to improve the model description for the overall charged multiplicity and the p_t distribution of the produced particles before we test the model efficiency against the different identified particle yields in AA collisions.

The SC-CR model increases the baryon production in pp and pPb collision systems. The result of strangeness enhancement in the strange

baryons sector without any assumption of thermalised medium opens the possibility for an alternative explanation for the observed strangeness enhancement in heavy-ion collisions. The results from heavy hyperons are much below the experimental observations (figure 14, but we should note that these results are producing a similar trend of strangeness enhancement to that of rope-hadronization [35]. We hope that in future combining these two models will improve the PYTHIA8/Angantyr model efficiency in reproducing the strange hadrons yield.

5 Discussion and outlook

We have here presented a first attempt to extend the concept of colour reconnections to apply also between sub-collisions in heavy ion events. This was done by modifying the QCD colour reconnection model in PYTHIA8 to limit the spatial distance between dipoles that are allowed to reconnect. This was done with a simple cutoff in impact parameter distance, δb_c , for which we found a value 0.5 fm, to give reasonable results.

This is clearly a quite naive approach, and the aim is mainly to understand the phenomenology of allowing inter-sub-collision CR in heavy ion collisions. There are many paths to improve our simple model. It is not unnatural, *e.g.*, to let the value of

δb_c depend on the local density of dipoles, and/or the transverse momentum of the partons involved in the reconnections. The role of m_0 also needs to be studied more, and this parameter could also be allowed to depend on such local features of the event. There are also other reconnection models that can be considered for use in heavy ion collisions, such as the perturbative swing model in Ref. [12, 23].

Our results are not perfect, but we still feel that they are encouraging. Introducing the cut-off makes the reproduction of pp minimum bias data worse than in default PYTHIA8, but not very much worse than what is obtained with the QCD-CR model. For pA collisions we get a reduced multiplicity, as expected, but we find that it can be compensated by modifying the treatment of secondary non-diffractive sub-collisions in the Angantyr model. Finally, we find that when extrapolating to full AA events we again obtain a too low multiplicity for central events, but the reduction is typically below 20%.

It should be remembered here that there are many other effects to consider, both in high-multiplicity pp collisions and in heavy ion collisions. In our group, we have considered so-called string shoving [10, 11] and rope hadronization [12], as well as hadronic rescattering [14]. Especially the latter would be interesting study together with colour reconnection in heavy ion collisions, since it has been found that rescattering typically increases the multiplicity for central collisions [15].

The QCD-CR model has shown enhanced production of the baryons compared to the default MPI-based CR model, which is purely a byproduct of junction systems. Hence, there may be some effects similar to strangeness enhancement due to the QCD-CR model in the baryon sector [41]. The QCD-CR model has shown effects similar to collectivity [42]. This work will also enable us to study and investigate the contribution of different event simulation stages like CR, string interactions (shoving and rope), and hadronic rescattering on the various final state observables in pp, pA, and AA collisions. In future work, we will show the results of the new implementation for the flavour production and collectivity-like behaviour in all three collision systems, namely pp, pA, and AA.

A top priority for future work is therefore to develop our implementation to allow the study of

the simultaneous effects of all these models. Only then one would be able to do a proper tuning of the involved parameters. In doing so we would again follow the procedure used here, *i.e.*, first tune to minimum bias pp observables of multiplicities and transverse momentum, and then adjust parameters that also depends on inter-sub-event effect by tuning to similar observables in pA in order to be able to have a parameter-free extrapolation to AA events.

Acknowledgments. We thank Gösta Gustafson, Torbjörn Sjöstrand and Christian Bierlich for interesting discussions and important input to this work.

This work was funded in part by the Knut and Alice Wallenberg foundation, contract number 2017.0036, Swedish Research Council, contracts numbers 2016-03291 and 2020-04869, in part by the European Research Council (ERC) under the European Union's Horizon 2020 research and innovation programme, grant agreement No 668679, and in part by the MCnetITN3 H2020 Marie Curie Initial Training Network, contract 722104.

Appendix A Junction Fragmentation

The hadronization in PYTHIA is done through Lund string fragmentation. PYTHIA has two methods for hadron production; string fragmentation and mini string fragmentation. Both are fundamentally based on the same mechanism, but the latter is an approximation for short strings (mini-strings), which becomes more important with many reconnections in HI events. Depending on the invariant mass of the colour singlet string/junction system, PYTHIA's algorithm selects one of the two methods to produce primary hadrons.

String fragmentation fragments long strings. For the junction systems, the algorithm fragments two lower energy junction legs first, and it starts from the lowest energy leg. The two low-energy junction legs are fragmented until every leg is left with a parton directly connected to the junction. Later, the two partons from these low-energy legs are combined to form a diquark (or anti-diquark). The diquark is then treated as one end of the remaining highest energy junction leg. At this

stage, the junction system no longer exists, and the last junction leg with a diquark at one end undergoes further string fragmentation as a normal string. Figure A1 shows the progress of the junction break-ups, formation of a diquark, and transformation of the junction system into a string system.

Mini-string fragmentation is used to hadronize short strings. It produces one or two hadrons depending on the energy in the string, and low-energy junction systems are not treated in the mini-string fragmentation. Prior to this work, if low-energy junction systems are found then such an event is aborted and a new event is generated. When we merged multiple pp-like events at the parton level in a HI event and tried to perform CR in the entire event, we observed enhancement in the number of junction systems, and many of them are below the invariant mass cut-off for string fragmentation. All those junction systems have to be fragmented within a mini-string fragmentation module, otherwise, the majority of HI events are aborted due to one or more untreated colour singlet systems in the hadronization stage. Hence, we developed two new fragmentation functions: "MiniJunct2Hadrons" and "MiniJunct2Baryons", in the mini-string fragmentation.

Before we provide an overview of the technical details of the two new functions, we like to discuss some additional constraints we introduced inside the QCD-CR model. We observe that most of these junction systems in pA and AA systems, have diquarks in the junction legs. Now, as we mentioned earlier, in the string fragmentation the two lower energy legs of a junction system are fragmented and the remainder is merged to form a string connecting the diquark with the highest energy junction leg. But in the case of the junction being connected to a diquark, it often occurs that either both or one of the low-energy legs is left with a diquark. PYTHIA can not merge such junction legs, where one or both legs have a diquark.

Sometimes, the highest energy leg also has a diquark at the end. Now, after merging two low-energy legs into a diquark, the string has a diquark at both ends. Although string fragmentation is a probabilistic mechanism and the strings with two diquarks may fragment successfully, sometimes they fail due to the last string piece being left with a diquark at both ends. The last piece

can not be hadronized as a tetra-quark system at this moment, although that could in principle be considered. We introduce an additional attempt by forwarding such a failed string fragmentation to mini-string fragmentation, where the string/junction system is forced to produce one or two hadrons.

To avoid recurring failures in the string fragmentation due to junction systems containing diquarks in pA and AA collisions, we do not allow dipoles with a diquark to undergo CR. This constraint is provided with a Boolean flag, so future users can test the options with or without allowing CR for diquarks containing dipoles. In pp collisions, another source of diquarks prior to string fragmentation is beam remnants. PYTHIA allows users to choose if the beam remnants may form a junction or a diquark with the remaining valance quarks of the beam remnant. Here, we choose junction formation to reduce the preexisting number of diquarks in the event during the CR. We continue to use this setup not only for pp collisions but also for pA and AA collisions.

Now, let's go back to the junctions in mini-string fragmentation. The first step is to check if the junction contains any gluons or not. If any of the junction legs have gluons, we reduce the junction system size by absorbing the gluons into the diquark or quark of the respective junction legs. The idea here is to simplify the next steps of producing hadrons via "junction collapse". We reduce the complex junction system to a simple junction system, where every leg contains only a quark or a diquark or respective anti-particle at its end. Now, we calculate the number of diquarks in the junction system. As shown in Figure A2, the junction can have up to three diquarks, when all the junction legs have a diquark. Depending on the number of diquarks, we have three possible outcomes for the junction to collapse and produce primary hadrons.

Case A (All the legs have quarks):

In this case, we follow the steps similar to the last stage of junction fragmentation in the string fragmentation mechanism. We merge the two lowest energy legs to form a diquark. Then we reduce the junction into a mini-string containing a diquark and a quark. After that, we use the existing mini string fragmentation functions to produce primary hadrons.

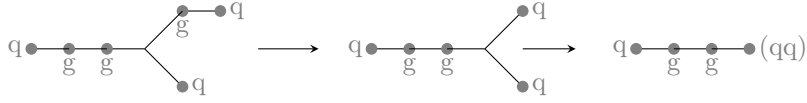


Fig. A1: Junction fragmentation steps. *Left:* A colour singlet junction system. In this example, the lowest energy leg is the one with a quark directly attached to the junction. The highest energy leg is the one with the longest chain of dipoles. *Centre:* The junction system after both the low-energy legs are fragmented and left with a quark directly connected to the junction. The highest energy leg is intact. *Right:* The final state of the junction system is shown. Here, the quarks of the two low-energy junction legs are combined to form a diquark (represented as (qq)), and it is attached at the end of the highest-energy leg. The remaining junction system is now replaced with a single string, and it will fragment according to the normal string fragmentation.

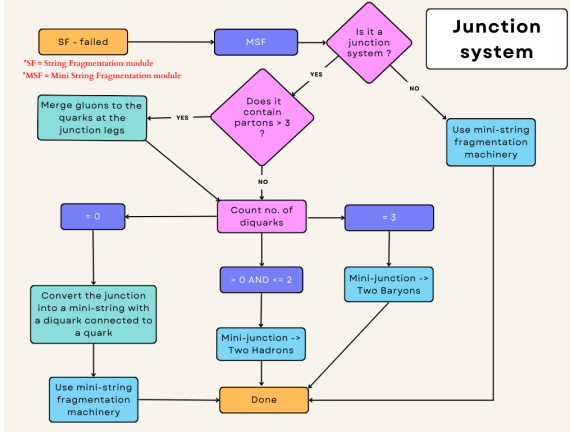


Fig. A2: Overview of the steps taken if the string fragmentation module fails to produce hadrons, and the handling of junction systems in the mini-string fragmentation to produce primary hadrons. The flow chart shows examples of cases with quarks and diquarks, but the junctions can also have anti-quarks and anti-diquarks.

Case B (The junction legs have a maximum of two diquarks):

Here, depending on whether the junction has one or two diquarks we collapse it to produce two mesons, or one baryon and one meson. We observed that the junctions containing one diquark have anti-quarks on the remaining legs and if it's an anti-diquark then quarks. Similarly, in the case of two diquarks, then the remaining leg has an anti-quark, and if two anti-diquarks then a quark. Hence, we treat the junction as a single entity containing a given number of diquarks, anti-diquarks, quarks and anti-quarks, and we produce hadrons accordingly.

Case B.1 (One diquark, and two anti-quarks):

Here, we break the diquark into two quarks. Then we pair each quark with a randomly selected anti-quark from the two anti-quarks. We check if the produced mesons have the correct quark flavours or not. Then we check if the sum of their masses is less than the invariant mass of the junction system or not. If the sum of the masses is below the junction system's invariant mass, then the mesons are assigned momenta as if a mother particle decays into the two daughter particles. If it fails then we repeat the process several times. If all attempts fail, the function returns a message about failed attempts, and the event is aborted.

Case B.2 (Two diquarks and one anti-quark):

Here, a diquark with the lowest invariant mass is broken into two quarks. One of the quarks is randomly selected and assigned to the other diquark, and the other quark is paired with the anti-quark. Again we check the flavours and compare the sum of the masses of the baryon and the meson with the junction system mass. If the sum of the masses is below the junction system's invariant mass then the hadrons are assigned momenta as if a mother particle decays into the two daughter particles. If it fails then we repeat the process several times. If all attempts fail, the function returns a message about failed attempts, and the event is aborted.

Case C (All legs have diquarks):

In this case, we have in total six quarks, and we collapse the junction to produce two baryons. We follow the procedure similar to case B.2, the diquark with the lowest invariant mass is split into two quarks. One of the quarks is randomly assigned to one of the remaining two diquarks. The rest of the steps are the same.

References

- [1] M. Gyulassy, L. McLerran, New forms of QCD matter discovered at RHIC. Nucl. Phys. A **750**, 30–63 (2005). <https://doi.org/10.1016/j.nuclphysa.2004.10.034>. arXiv:nucl-th/0405013
- [2] J.A. et al. (ALICE collaboration), Enhanced production of multi-strange hadrons in high-multiplicity proton-proton collisions. Nature Phys. **13**(535) (2017). arXiv:1606.07424
- [3] V.K. et al. (CMS collaboration), Evidence for collectivity in pp collisions at the LHC. Phys. Lett.B. **765**(193) (2017). arXiv:1606.06198
- [4] T. Sjöstrand, S. Ask, J.R. Christiansen, R. Corke, N. Desai, P.I. et al., An introduction to pythia 8.2. Comput. Phys. Commun. **191**, 159 (2015). <https://doi.org/10.1016/j.cpc.2015.07.025>
- [5] C. Bierlich, et al., A comprehensive guide to the physics and usage of PYTHIA 8.3 (2022). arXiv:2203.11601 [hep-ph]
- [6] C. Bierlich, G. Gustafson, L. Lönnblad, H. Shah, The Angantyr model for Heavy-Ion Collisions in PYTHIA8. JHEP **10**, 134 (2018). [https://doi.org/10.1007/JHEP10\(2018\)134](https://doi.org/10.1007/JHEP10(2018)134). arXiv:1806.10820 [hep-ph]
- [7] R. Glauber, Cross sections in deuterium at high energies. Physical Review **100**(1), 242–248 (1955)
- [8] M.L. Miller, K. Reygers, S.J. Sanders, P. Steinberg, Glauber modeling in high energy nuclear collisions. Ann.Rev.Nucl.Part.Sci. **57**, 205–243 (2007). <https://doi.org/10.1146/annurev.nucl.57.090506.123020>
- [9] M.L. Good, W.D. Walker, Diffraction dissociation of beam particles. Phys. Rev. **120**, 1857–1860 (1960)
- [10] C. Bierlich, G. Gustafson, L. Lönnblad. A shoving model for collectivity in hadronic collisions (2016)
- [11] C. Bierlich, S. Chakraborty, G. Gustafson, L. Lönnblad, Setting the string shoving picture in a new frame. JHEP **03**, 270 (2021). [https://doi.org/10.1007/JHEP03\(2021\)270](https://doi.org/10.1007/JHEP03(2021)270). arXiv:2010.07595 [hep-ph]
- [12] C. Bierlich, G. Gustafson, L. Lönnblad, A. Tarasov, Effects of Overlapping Strings in pp Collisions. JHEP **03**, 148 (2015). [https://doi.org/10.1007/JHEP03\(2015\)148](https://doi.org/10.1007/JHEP03(2015)148). arXiv:1412.6259 [hep-ph]
- [13] C. Bierlich, Rope Hadronization and Strange Particle Production. EPJ Web Conf. **171**, 14,003 (2018). <https://doi.org/10.1051/epjconf/201817114003>. arXiv:1710.04464 [nucl-th]
- [14] T. Sjöstrand, M. Utheim, A Framework for Hadronic Rescattering in pp Collisions. Eur. Phys. J. C **80**(10), 907 (2020). <https://doi.org/10.1140/epjc/s10052-020-8399-3>. arXiv:2005.05658 [hep-ph]
- [15] C. Bierlich, T. Sjöstrand, M. Utheim, Hadronic rescattering in pA and AA collisions. Eur. Phys. J. A **57**(7), 227 (2021). <https://doi.org/10.1140/epja/s10050-021-00543-3>. arXiv:2103.09665 [hep-ph]
- [16] T. Sjöstrand, M. van Zijl, A multiple interaction model for the event structure in hadron collisions. Phys. Rev. **D36** (1987). <https://doi.org/10.1103/PhysRevD.36.1300>
- [17] J.R. Christiansen, P.Z. Skands, String Formation Beyond Leading Colour. JHEP **08**, 003 (2015). [https://doi.org/10.1007/JHEP08\(2015\)003](https://doi.org/10.1007/JHEP08(2015)003). arXiv:1505.01681 [hep-ph]
- [18] A. Breakstone, et al., Multiplicity Dependence of Transverse Momentum Spectra at ISR Energies. Phys. Lett. B **132**, 463–466 (1983). [https://doi.org/10.1016/0370-2693\(83\)90348-9](https://doi.org/10.1016/0370-2693(83)90348-9)
- [19] C. Albajar, et al., A Study of the General Characteristics of $p\bar{p}$ Collisions at $\sqrt{s} = 0.2\text{-TeV}$ to 0.9-TeV . Nucl. Phys. B **335**,

- 261–287 (1990). [https://doi.org/10.1016/0550-3213\(90\)90493-W](https://doi.org/10.1016/0550-3213(90)90493-W)
- [20] G. Gustafson, U. Pettersson, P.M. Zerwas, Jet Final States in W W Pair Production and Color Screening in the QCD Vacuum. *Phys. Lett. B* **209**, 90–94 (1988). [https://doi.org/10.1016/0370-2693\(88\)91836-9](https://doi.org/10.1016/0370-2693(88)91836-9)
- [21] T. Sjöstrand, V.A. Khoze, On Color rearrangement in hadronic W⁺ W⁻ events. *Z. Phys. C* **62**, 281–310 (1994). <https://doi.org/10.1007/BF01560244>. [arXiv:hep-ph/9310242](https://arxiv.org/abs/hep-ph/9310242)
- [22] G. Gustafson, J. Häkkinen, Color interference and confinement effects in W pair production. *Z. Phys. C* **64**, 659–664 (1994). <https://doi.org/10.1007/BF01957774>
- [23] L. Lönnblad, Reconnecting colored dipoles. *Z. Phys. C* **70**, 107–114 (1996). <https://doi.org/10.1007/s002880050087>
- [24] C. Friberg, G. Gustafson, J. Häkkinen, Color connections in e⁺ e⁻ annihilation. *Nucl. Phys. B* **490**, 289–305 (1997). [https://doi.org/10.1016/S0550-3213\(97\)00064-3](https://doi.org/10.1016/S0550-3213(97)00064-3). [arXiv:hep-ph/9604347](https://arxiv.org/abs/hep-ph/9604347)
- [25] B. Andersson, P. Dahlqvist, G. Gustafson, ON LOCAL PARTON HADRON DUALITY. 1. MULTIPLICITY. *Z. Phys. C* **44**, 455 (1989). <https://doi.org/10.1007/BF01415560>
- [26] V. Khachatryan, et al., Charged Particle Multiplicities in pp Interactions at $\sqrt{s} = 0.9, 2.36$, and 7 TeV. *JHEP* **01**, 079 (2011). [https://doi.org/10.1007/JHEP01\(2011\)079](https://doi.org/10.1007/JHEP01(2011)079). [arXiv:1011.5531](https://arxiv.org/abs/1011.5531) [hep-ex]
- [27] G. Aad, et al., Charged-particle multiplicities in pp interactions measured with the ATLAS detector at the LHC. *New J. Phys.* **13**, 053,033 (2011). <https://doi.org/10.1088/1367-2630/13/5/053033>. [arXiv:1012.5104](https://arxiv.org/abs/1012.5104) [hep-ex]
- [28] T. Sjöstrand, P.Z. Skands, Baryon number violation and string topologies. *Nucl. Phys. B* **659**, 243 (2003). [https://doi.org/10.1016/S0550-3213\(03\)00193-7](https://doi.org/10.1016/S0550-3213(03)00193-7). [arXiv:hep-ph/0212264](https://arxiv.org/abs/hep-ph/0212264)
- [29] G.A. Schuler, T. Sjöstrand, Hadronic diffractive cross-sections and the rise of the total cross-section. *Phys. Rev. D* **49**, 2257–2267 (1994). <https://doi.org/10.1103/PhysRevD.49.2257>
- [30] E.L. Berger, J.C. Collins, D.E. Soper, G.F. Sterman, Diffractive Hard Scattering. *Nucl. Phys. B* **286**, 704–728 (1987). [https://doi.org/10.1016/0550-3213\(87\)90460-3](https://doi.org/10.1016/0550-3213(87)90460-3)
- [31] K.H. Streng, in *DESY Workshop 1987: Physics at HERA* (1988)
- [32] A. Buckley, H. Hoeth, H. Lacker, H. Schulz, J.E. von Seggern, Systematic event generator tuning for the LHC. *Eur. Phys. J. C* **65**, 331–357 (2010). <https://doi.org/10.1140/epjc/s10052-009-1196-7>. [arXiv:0907.2973](https://arxiv.org/abs/0907.2973) [hep-ph]
- [33] V. Khachatryan, et al., Transverse-momentum and pseudorapidity distributions of charged hadrons in pp collisions at $\sqrt{s} = 7$ TeV. *Phys. Rev. Lett.* **105**, 022,002 (2010). <https://doi.org/10.1103/PhysRevLett.105.022002>. [arXiv:1005.3299](https://arxiv.org/abs/1005.3299) [hep-ex]
- [34] J. Adam, et al., Enhanced production of multi-strange hadrons in high-multiplicity proton-proton collisions. *Nature Phys.* **13**, 535–539 (2017). <https://doi.org/10.1038/nphys4111>. [arXiv:1606.07424](https://arxiv.org/abs/1606.07424) [nucl-ex]
- [35] C. Bierlich, S. Chakraborty, G. Gustafson, L. Lönnblad, Strangeness enhancement across collision systems without a plasma. *Phys. Lett. B* **835**, 137,571 (2022). <https://doi.org/10.1016/j.physletb.2022.137571>. [arXiv:2205.11170](https://arxiv.org/abs/2205.11170) [hep-ph]
- [36] G. Aad, et al., Measurement of the centrality dependence of the charged-particle pseudorapidity distribution in proton–lead collisions at $\sqrt{s_{NN}} = 5.02$ TeV with the ATLAS detector. *Eur. Phys. J. C* **76**(4), 199 (2016). <https://doi.org/10.1140/epjc/s10052-016-4002-3>. [arXiv:1508.00848](https://arxiv.org/abs/1508.00848) [hep-ex]
- [37] C. Bierlich, et al., Confronting experimental data with heavy-ion models: RIVET for heavy ions. *Eur. Phys. J. C* **80**(5),

485 (2020). <https://doi.org/10.1140/epjc/s10052-020-8033-4>. arXiv:2001.10737 [hep-ph]

- [38] B.B. Abelev, et al., Multiplicity Dependence of Pion, Kaon, Proton and Lambda Production in p-Pb Collisions at $\sqrt{s_{NN}} = 5.02$ TeV. Phys. Lett. B **728**, 25–38 (2014). <https://doi.org/10.1016/j.physletb.2013.11.020>. arXiv:1307.6796 [nucl-ex]
- [39] K. Aamodt, et al., Centrality dependence of the charged-particle multiplicity density at mid-rapidity in Pb-Pb collisions at $\sqrt{s_{NN}} = 2.76$ TeV. Phys. Rev. Lett. **106**, 032,301 (2011). <https://doi.org/10.1103/PhysRevLett.106.032301>. arXiv:1012.1657 [nucl-ex]
- [40] G. Aad, et al., Measurement of charged-particle spectra in Pb+Pb collisions at $\sqrt{s_{NN}} = 2.76$ TeV with the ATLAS detector at the LHC. JHEP **09**, 050 (2015). [https://doi.org/10.1007/JHEP09\(2015\)050](https://doi.org/10.1007/JHEP09(2015)050). arXiv:1504.04337 [hep-ex]
- [41] C. Bierlich, J.R. Christiansen, Effects of color reconnection on hadron flavor observables. Phys. Rev. D **92**(9), 094,010 (2015). <https://doi.org/10.1103/PhysRevD.92.094010>. arXiv:1507.02091 [hep-ph]
- [42] A. Ortiz Velasquez, P. Christiansen, E. Cuautle Flores, I. Maldonado Cervantes, G. Paic, Color Reconnection and Flowlike Patterns in pp Collisions. Phys. Rev. Lett. **111**(4), 042,001 (2013). <https://doi.org/10.1103/PhysRevLett.111.042001>. arXiv:1303.6326 [hep-ph]